1998, Vol. 24, No. 5, 1315–1341

A Shape-Contrast Effect for Briefly Presented Stimuli

Satoru Suzuki
University of Arizona

Patrick Cavanagh
Harvard University

When a suprathreshold visual stimulus is flashed for 60–300 ms and masked, though it is no longer visibly degraded, the perceived shape is vulnerable to distortion effects, especially when a 2nd shape is present. Specifically, when preceded by a flashed line, a briefly flashed circle appears to be an ellipse elongated perpendicular to the line. Given an appropriate stimulus onset asynchrony, this distortion is perceived when the 2 stimuli (~4°) are presented as far as 12° apart but is not due to perception of apparent motion between the 2 stimuli. Additional pairs of shapes defined by taper and overall curvature also revealed similar nonlocal shape distortion effects. The test shapes always appeared to be more dissimilar to the priming shapes, a distortion termed a *shape-contrast effect.* Its properties are consistent with the response characteristics of the shape-tuned neurons in the inferotemporal cortex and may reveal the underlying dimensions of early shape encoding.

From the instant a stimulus is presented, the visual system accumulates information about the stimulus and begins to generate a subjective impression of its shape and location. For very brief presentations terminated by a mask, stimuli look fuzzy, ill defined, or intertwined with the details of the mask. Several studies have shown that for durations greater than ~50 ms, the stimulus begins to have a relatively sharp, crisp appearance and is seen independently of the mask (e.g., Eriksen & Hoffman, 1963; Georgeson, 1988; Georgeson & Georgeson, 1987; Rolls, Tovee, Purcell, Stewart, & Azzopardi, 1994; Turvey, 1973). However, we find that even if the stimulus appears to be seen clearly, its apparent shape at moderately brief durations (50–300 ms) is quite "labile" (Experiment 1) and vulnerable to distortions generated by other stimuli in the field (Experiments 2–10). The accumulated information seems to be sufficient for generating sharply defined contours, but the remaining noise or uncertainty manifests itself as "structural noise," as opposed to image (or pixel) noise (e.g., Pelli, 1990). With longer delays before the mask (say, 300 ms), the percept of shape becomes increasingly veridical.

In the experiments reported in this article, we extensively investigated the properties of this intermediate, labile stage of visual processing. We demonstrate that it offers a psychophysical window into high-level visual processing in which images are coded in figural dimensions independently of spatial parameters.

The general paradigm used involved a priming stimulus, a test stimulus, and a random-dot mask. The priming stimulus was flashed first, followed by the test stimulus after some stimulus onset asynchrony (SOA), and then the mask. The main parameters manipulated were the shapes of the priming stimulus and the test stimulus, the distance between them their spatial orientation relative to each other, the SOA between them, and their eccentricities. To investigate the labile stage of shape processing, we kept the test stimulus duration brief (under 100 ms) in most experiments reported.

Our main finding, given that the test stimulus presentation is brief (the exposure duration was varied in Experiment 5) is that the priming stimulus distorts the perceived shape of the test stimulus in such a way that the latter appears more dissimilar to the former—a *shape-contrast effect.* The distortion effects turned out to be largely independent of spatial parameters such as the distance between the priming stimulus and the test stimulus, and their spatial configuration, given that the prime-to-test interval was ~200 ms (see Experiments 3, 9, and 10). Control conditions (see Experiments 4, 9, and 10) ruled out the possibility that the distortion effects were due to perception of apparent motion between the priming stimulus and the test stimulus. These results imply that when a test stimulus is presented briefly and rapidly following a priming stimulus, the priming stimulus influences the perceived shape of the test stimulus at the level of visual representation where the coding of images is shape specific but nonretinotopic (or nonlocal). We suggest that the shape-contrast effects demonstrated here may be a manifestation of neural interactions in higher visual areas such as the inferior temporal cortex (IT) and the superior temporal sulcus (STS), where neural codings are shape specific but no longer retinotopic.

Many neurons in those areas have nonretinotopic tuning for a variety of shapes such as 3-D head orientation (e.g., Perret et al., 1991), facial expression (e.g., Hasselmo, Rolls & Baylis, 1989), face shape (e.g., Perret et al., 1984; Young

Satoru Suzuki, Department of Psychology, University of Arizona; Patrick Cavanagh, Department of Psychology, Harvard University.

This research was supported by Air Force Office for Scientific Research Grant AFOSR 0189 and by Grant JSPS 3214 from the Japan Society for the Promotion of Science.

We thank Thomas Sanocki and two anonymous reviewers for their numerous comments and suggestions, which improved the article considerably. We are also grateful to those who participated in the experiments for their patience while spending many hours in front of the computer doing repetitive tasks.

Correspondence concerning this article should be addressed to Satoru Suzuki, who is now at the Department of Psychology, Northwestern University, 2029 Sheridan Road, Evanston, Illinois 60208. Electronic mail may be sent to satoru@nwu.edu.

& Yamane, 1992), and simple geometric shapes (e.g., Fujita, Tanaka, Ito, & Cheng, 1992; Tanaka, 1996). An important characteristic of these neurons is that their responses are nonlocal. The receptive fields of these neurons cover almost the entire visual field (e.g., Desimone & Gross, 1979; Gross, Rocha-Miranda, & Bender, 1972), so they respond to preferred shapes almost anywhere in the visual field. It is reasonable to expect that neural interactions at this level of processing might produce shape-specific but nonretinotopic distortions, just as classic aftereffects, which are local, are believed to be caused by neural interactions at lower levels of visual processing, where visual neurons have retinotopic receptive fields. We present the following brief review of classic aftereffects to point out important similarities and differences between those aftereffects and the shape-contrast effect we report in this article.

It is well known that prolonged viewing of a visual stimulus (adapting stimulus) distorts a subsequently viewed stimulus (test stimulus) given that the two stimuli are similar.[1] The phenomenon is commonly called a visual aftereffect. The distortion generally makes the test stimulus appear more dissimilar to the adapting stimulus. For example, adapting to a linear grating tilted slightly to the left makes a vertical test grating appear tilted slightly to the right—the tilt aftereffect (e.g., Blakemore & Campbell, 1969). Adapting to a grating of a certain spatial frequency makes a test grating of a slightly lower spatial frequency appear even coarser, and that of a slightly higher spatial frequency appear even finer[2]—the size/spatial-frequency aftereffect (e.g., Blakemore & Campbell, 1969; Blakemore, Nachmias, & Sutton, 1970). Adapting to a stimulus in one location makes a test stimulus presented slightly away from it appear even further away—the figural aftereffect (e.g., Kohler & Wallach, 1944; Sagara & Ohyama, 1957). Finally, prolonged viewing of one direction of motion makes a stationary stimulus appear to be moving in the opposite direction—the motion aftereffect (e.g., Anstis & Moulden, 1970; Wohlgemuth, 1911). An important characteristic of these aftereffects is that they are strictly local (except for some size aftereffects—e.g., Ohyama, 1954, 1956; Sagara & Ohyama, 1957—and some motion aftereffects—e.g., Culham & Cavanagh, 1995; von Grünau & Dube, 1992); test stimuli have to be presented at (or very near) the site of adaptation in order to obtain the effect.

These aftereffects have been thought to support the idea that perception of orientation, size/spatial frequency, position, and direction of motion are coded in the patterns of population activity of the sets of visual neurons that are locally and selectively tuned to the corresponding features. For example, visual neurons in the striate cortex are locally tuned to various orientations (e.g., Hubel & Weisel, 1968) and size/spatial frequencies (e.g., De Valois, Albrecht, & Thorell, 1982); they could thus code perception of local orientation and size/spatial frequency, and their selective adaptation could mediate tilt and size/spatial-frequency aftereffects. Similarly, neurons in MT (the medial temporal area; e.g., Albright, Desimone, & Gross, 1984; Movshon, Adelson, Gizzi, & Newsome, 1985) and MST (the medial superior temporal area; e.g., Graziano, Andersen, & Snowden, 1994; Lagae, Maes, Raiguel, & Xiao, 1994; Tanaka & Saito, 1989) are selectively tuned to various directions of motion (translation, expansion–contraction, rotation, etc.); evidence suggests that neurons in MT are intimately involved in determining the perceived directions of motion (Newsome, Britten, & Movshon, 1989) and mediate motion aftereffects (Tootell, Reppas, Dale, & Look, 1995). Reported spatial tolerance of some motion aftereffects (e.g., Culham & Cavanagh, 1995; von Grünau & Dube, 1992) might reflect the fact that visual neurons in MT and MST have large receptive fields. Any set of neurons with retinotopic receptive fields could code perceived location and mediate figural aftereffects (see Felleman & Van Essen, 1991, for degrees of preservation of retinotopy in various cortical visual areas).

The repulsive direction of these classic aftereffects has been explained by postulating that adaptation selectively reduces the sensitivity of neurons responsive to the adapting stimulus (e.g., Petersen, Baker, & Allman, 1985; Saul & Cynader, 1989a, 1989b). As a result, the "adapted" neurons make reduced responses to the subsequent test stimulus. This causes the overall (population) neural response pattern for the test stimulus to skew away from the adapting stimulus and thus produces a repulsive aftereffect.

If the nonretinotopic shape-selective neurons in the temporal areas interact in a manner similar to the largely retinotopic neurons responsible for classic aftereffects, a nonretinotopic shape aftereffect might be expected. Adapting to one shape would make a test shape appear more dissimilar to the adapting shape regardless of the retinal parameters such as distance between the two stimuli and their spatial orientation to each other. Such aftereffects may not have been reported before because the interactions among the shape-selective neurons might be too weak or too fleeting to result in discernible distortions of test stimuli under normal viewing conditions.

In this study, we revealed such shape-contrast effects using a technique of brief test presentation such that test stimuli were perceived at the labile stage of processing discussed earlier. We argue that this technique provides a sensitive way to detect weak and fleeting interactions between the neural units at the level of shape processing. Others have provided previous examples of accentuated distortion effects with brief tests. Wolfe (1984) demonstrated that the classic tilt aftereffect has a strong component that decreases rapidly with longer test duration, dropping to the level of the conventional tilt aftereffect at large exposure durations (>500 ms). In a previous study (Suzuki & Cavanagh, 1997) we demonstrated repulsive effects of focused attention that could be seen only with briefly flashed position-probes.

The rest of the article is devoted to (a) providing psychophysical evidence for the existence of nonretinotopic shape-contrast effects above and beyond the effects of low-level contour interactions (figural aftereffects; e.g., Fox, 1951; Kohler & Wallach, 1944; Sagara & Ohyama, 1957) and shape-changing apparent motion (representational mo-

[1] Similar in the sense that the two stimuli activate a common set of visual neurons.

[2] Given that the adapting grating and the test grating have similar orientations.

mentum; e.g., Finke & Shyi, 1988; Freyd & Johnson, 1987; Kelly & Freyd, 1987) and (b) exploring in detail the spatial and temporal characteristics of these distortion effects.

The first pair of stimuli whose shape interaction we chose to test consisted of a line (as the priming stimulus) and a circle (as the test stimulus); we chose these stimuli partly because of the historical use of them and partly because people are sensitive in detecting slight distortion effects on a circle (e.g., Regan & Hamstra, 1992). Kohler and Wallach (1944) reported that a prolonged adaptation to an ellipse makes a subsequently viewed circle presented at the same location appear distorted into an ellipse perpendicular to the adapting ellipse (also see Regan & Hamstra, 1992, for a comprehensive study of aspect-ratio-based aftereffects). Hartmann (1923/1955), using briefly presented stimuli, observed a similar phenomenon that is more related to the present study. He flashed a line and a smaller circle in a rapid succession, centered at the same location. He found a distortion effect similar to that found by Kohler and Wallach (i.e., considering a line an infinitely flattened ellipse); a flashed line makes a subsequently flashed circle at the same location appear distorted into an ellipse perpendicular to the line. However, in addition to reporting the distortion effect, Hartmann noted that the line appeared to dynamically deform into the circle. In particular, the line terminators appeared to move inward, squashing the circle, while the portion of the line within the circle appeared to move outward, stretching the circle. He argued that those movements were responsible for the observed distortion effect (see Figure 1).

In Experiment 2 we rejected this motion-extrapolation hypothesis and a size-aftereffect explanation of the distortion effect. In Experiment 3 we demonstrated that the same shape distortion occurs even if the two stimuli are presented at different locations and regardless of their spatial configuration, which suggests the nonretinotopic nature of the distortion effect. In Experiment 4 we showed that the distortion effect is not due to the perception of apparent motion between the priming line and the test circle. In Experiments 5 and 6, we varied the "signal strength" of the test stimulus in a variety of ways (by varying the test stimulus duration, eccentricity, and contrast) and showed that the distortion effect is generally stronger when the test stimulus is weaker. We examined the effect of the prime-to-test SOA when the priming stimulus and the test stimulus were presented at the same location (Experiment 7) and when the two stimuli were presented at separate locations (Experiment 8). The results showed that the distortion effect depends critically on the spatiotemporal proximity between the two interacting shapes.

Finally, to test the idea that the shape-contrast effect is a general phenomenon and not unique to the interactions between lines and circles, we tested two additional pairs of more complex shapes in Experiment 9 (a triangle on a square) and Experiment 10 (a mouthlike shape with net curvature on a flattened diamond with no net curvature). Those stimuli were designed such that low-level contour interactions would predict no systematic shape distortion effects. Both pairs of shapes yielded nonretinotopic distortion effects of a shape-contrast nature; the test shape was distorted in such a way that it appeared more dissimilar in overall shape to the priming shape regardless of the spatial configuration of the interacting shapes.

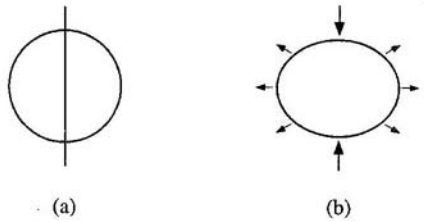

Figure 1. The motion-extrapolation hypothesis of the distortion effect (Hartmann, 1923/1955). (a) The line is flashed prior to the circle. (b) The shape-changing movements seen are the salient contractile movements of the line terminators (big arrows) and the less salient expansive movements of the linear contour inside the circle (small arrows). Hartmann claimed that these movements are responsible for the observed shape distortion effect (squashing).

General Method

The basic paradigm is shown in Figure 2. A line is flashed (30 ms) randomly in one of the quadrants. The line is oriented either vertically or horizontally.[3] Following an SOA of 180 ms, a circle is flashed (60 ms) at the overlapping location, followed by a random-dot mask (255 ms). It turns out that the circle appears elongated into an ellipse whose major axis is perpendicular to the priming line.

All stimuli were displayed on a 13-in. (33-cm) color monitor (66 Hz), and all experiments were controlled with a Macintosh IIcx computer with the software Shell & Macglib (micro ML Inc., Quebec, Canada). The experiments were conducted in a dimly lit room, and the observers were tested individually. Undergraduate students, graduate students, and postdoctoral fellows from Harvard University and the University of Arizona participated in the experiments. Observers A.B., C.H., S.G., and T.H. were undergraduate students who were not previously trained in psychophysical experiments and were paid to participate in the experiments. S.S. is one of the authors. The rest of the observers were graduate students and postdoctoral fellows in experimental psychology who volunteered to participate but were naive as to the specific hypotheses tested in the experiments. All observers had normal or corrected-to-normal vision. In all experiments except for Experiments 4, 9, and 10, the observer was seated 46 cm from the monitor (such that each pixel subtended 2.7′ of visual angle) and a chin rest was used to restrain head movements. For technical reasons, no chin rest was used in Experiments 4, 9, and 10 and the observer was seated about 50 cm from the monitor; thus, the stimuli were slightly scaled down (about 10%) in those experiments. The priming stimuli (9.1 cd/m^2)—lines (Experiments 2–8), triangles (Experiment 9), and mouthlike shapes (Experiment 10)—and the test stimuli (3.7

[3] A pilot study showed that qualitatively the same distortion effects are obtained with other orientations of the line. In fact, the effect appears to be larger when the line orientation is other than vertical or horizontal. We plan to investigate this potential "oblique-superiority" phenomenon in a follow-up study. The magnitude of the distortion effect also seems to vary noticeably from trial to trial. In this article, we report the distortion effects as averaged over many trials for the purpose of characterizing their dependences on spatial and temporal parameters. An investigation into the cause of their trial-to-trial fluctuation is currently under way.

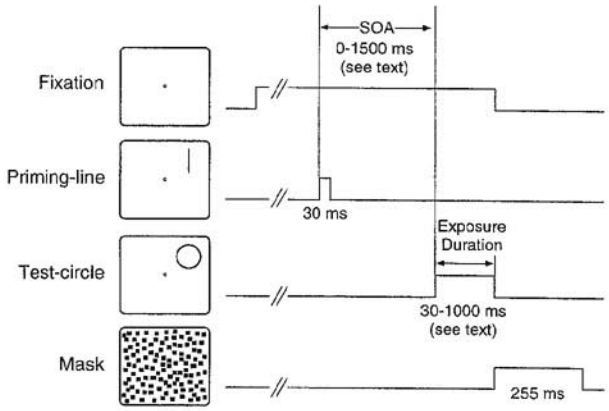

Figure 2. Basic trial events for Experiments 2–3 and 5–8, which demonstrate the line-on-circle shape distortion effect. The priming line and the test circle were presented at overlapping locations in Experiments 2, 5, 6, and 7. The distance between the line and the circle was varied in Experiment 3. The two stimuli were separated by a fixed distance in Experiment 8. SOA = stimulus onset asynchrony.

cd/m^2)—circles (Experiments 2–8), ellipses (for the control experiment, Experiment 1), squares (Experiment 9), and flattened diamonds (Experiment 10)—were presented against a dark background (0.02 cd/m^2). The observer always viewed a small fixation circle (1.85 cd/m^2; 0.18° in diameter) located at the center of the monitor. All stimuli were drawn with 1-pixel (2.7′) wide curves, except for the priming shapes used in Experiments 4, 9, and 10, which were drawn with curves three times as thick in order to make their movement more salient in the motion conditions (see corresponding *Method* sections for more detail). A random-dot field of 1-pixel squares was used as the mask; the bright squares (53.3 cd/m^2) randomly covered 50% of the screen in each trial.[4]

At the beginning of each trial, a fixation circle appeared at the center of the screen at the sound of a warning beep; the observer fixated the fixation circle for 1,800 ms before the trial events started. The observer was instructed to maintain fixation throughout the trial (except during the mask).

A two-parameter matching technique (method of adjustment) was used to measure the amount of stimulus deformation in all experiments in which distortion effects of a line on a circle were measured (Experiments 2 through 8). A less rigorous one-parameter matching technique was used to measure the distortion effect of a triangle on a square (Experiment 9). We used a two-alternative forced-choice paradigm to examine interactions between a mouthlike shape with net curvature and a flattened diamond with no net curvature (Experiment 10). In all experiments, some practice trials were given prior to the experimental trials so that the observer could get used to the trial events and the experimental procedure.

Because we intended to examine the spatial and temporal characteristics of the distortion effects for the interactions between a line and a circle in detail, we first conducted a control experiment to evaluate the sensitivity of our two-parameter matching method. In the actual line-on-circle distortion experiments (Experiments 2–8), the observers reproduced the shape of the test circle as they saw it (a vertically or horizontally elongated ellipse[5]) on the computer screen. At the end of each trial, the matching stimulus was presented at the center of the computer screen; it was initially a perfect circle identical to the flashed circle (3.8° in diameter). The observer distorted the matching circle by manipulating the lengths of its vertical and horizontal diameters by moving the computer mouse in vertical and horizontal directions, respectively. Upward/downward movement of the mouse increased/decreased the vertical diameter, whereas rightward/leftward movement increased/decreased the horizontal diameter. The lengths of the two diameters were recorded when the observer believed he or she successfully reproduced the distorted test circle and double-clicked the mouse.

Two quantities were computed from these values. One was an index of the degree of elongation of the reproduced ellipse. It was computed by dividing the difference between the two diameters by the shorter diameter and multiplying by 100: ([longer diameter] − [shorter diameter])/(shorter diameter) × 100. The value thus computed indicates the percentage by which the longer diameter is longer relative to the shorter diameter; we call it percent elongation. For example, a 0% elongation would indicate a perfect circle, whereas a 50% elongation would indicate an ellipse with a longer diameter that is 50% longer than its shorter diameter. A larger value corresponds to an ellipse with proportionally greater elongation. A positive sign was given if the orientation of the reproduced ellipse was perpendicular to that of the priming line; otherwise (i.e., if the orientation of the reproduced ellipse was the same as that of the priming line), a negative sign was given. Thus, for the measurement of the distortion effect, a larger positive value of percent elongation indicated a larger amount of the effect in the predicted direction (the test circle being distorted into an ellipse oriented perpendicular to the preceding priming line).

The second quantity computed was the area of the reproduced ellipse. It was obtained with the usual formula: (longer diameter) × (shorter diameter) × (π/4).

In the control experiment (Experiment 1), we tested the reliability of this matching method by flashing horizontal and vertical ellipses of various degrees of elongation (or aspect ratios) one at a time with no priming line; we measured how well the observer reproduced those ellipses of known degrees of elongation. In this case, the percent elongation value received a positive sign if the orientation of the reproduced ellipse was the same as that of the presented ellipse; otherwise (i.e., if the orientation of the reproduced ellipse was perpendicular to that of the presented ellipse), a negative sign was given. The result of this experiment determined the relationship between the observer's estimates and the actual elongation (or aspect ratio) of briefly flashed ellipses. For the matching technique to be useful, the relationship between the reproduced and the actual degrees of elongation must be at least monotonic; a high linear correlation is desired.

Experiment 1: Test of the Reliability of the Matching Technique

In this experiment, horizontally and vertically oriented ellipses of various degrees of elongation were flashed one at a time in a peripheral field (6.5° eccentricity). The exposure duration was varied as well. The observer's estimates of the

[4] For clarity of reproduction, the luminance polarity of the stimuli is reversed (black on white) in Figures 2, 7, 8, 9, 12, 18, 19, 20, 22, 23, 24, and 25. Furthermore, note that the mask is depicted with disproportionately large dark pixels in Figures 2, 12, 20, and 24.

[5] Because the priming line was always vertically or horizontally oriented, the distortion effect on the test circle was always horizontal or vertical elongation.

ellipses' elongation obtained with the matching technique (described previously) were compared with the corresponding actual values. The aim of this experiment was twofold. The first aim was to verify a high correlation between the reproduced and the actual degrees of elongation in order to justify the use of the matching technique in the subsequent experiments. The second aim was to find any perceptual bias shown by observers in perceiving briefly flashed ellipses. In particular, Lindermann (1922/1955) reported that briefly presented ellipses (including circles) produced a sensation of motion. When the exposure duration was in the range of 35–220 ms, some observers saw the ellipses expanding as they appeared and contracting as they disappeared. Those observers who saw this type of motion estimated the initial size of the flashed ellipses to be smaller than the resting size, growing larger toward the end of the expansion phase and then smaller again during the contraction phase. Furthermore, the expansion for Lindermann's observers always appeared greater in the horizontal than in the vertical direction; as a result, the ellipses always appeared slightly elongated in the horizontal direction (relative to their veridical shapes). In our experiment, the contracting phase of this size/shape-changing motion was unlikely to be observed because of the use of backward masking. In fact, none of our observers reported any salient contour movements interfering with their task.

Method

Observers. Five observers participated in the experiment.

Stimuli. The flashed ellipse had a diameter of 3.8° when it was a circle (elongation = 0%). The ellipses of other degrees of elongation were created by increasing the length of one major axis and decreasing the length of the other by the same amount; this procedure kept the area constant within 0.4% while the degree of elongation was varied from 0.0 to 13.0%. The stimulus eccentricity was 6.5° at the center. Also see the General Method section.

Procedure. A vertically or horizontally oriented ellipse of a variable degree of elongation (0–13%) was flashed for a variable duration (30–1,000 ms), randomly in the middle of one of the quadrants, and was immediately followed by the random-dot mask (255 ms). The observer recreated the ellipse he or she saw by using the matching technique (see the General Method section).

Each observer was given three blocks of 280 trials: (2 ellipse orientations) × (5 levels of elongation) × (7 exposure durations) × (4 quadrants). The order of the trials was randomized for each block for each observer. A short break was given every 70 trials. The first block was a practice block; the data from the latter two blocks (a total of 560 trials) were analyzed.

Results and Discussion

In Figure 3a, the reproduced degree of elongation (%) is plotted as a function of the actual degree of elongation (%) of the flashed ellipse (collapsed over exposure duration). The thin curves are the data from the individual observers, and the thick curve is the mean. The error bars are the standard errors of the mean with the variance that is due to the horizontal bias removed (this is explained a little further on). It is obvious from Figure 3a that the reproduced degree of elongation is linearly correlated with the actual value;

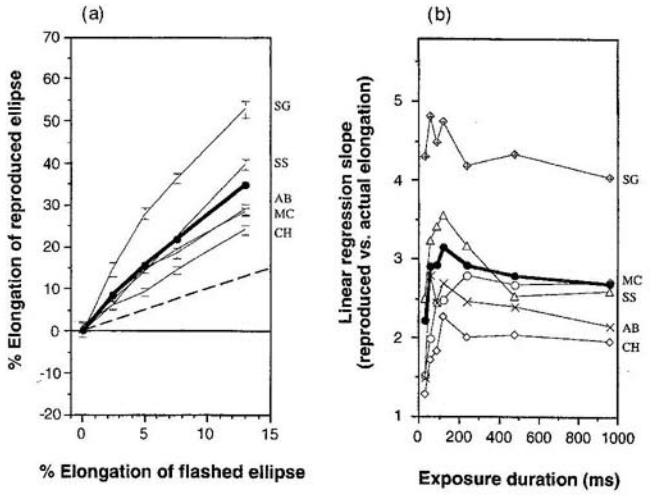

Figure 3. (a) The reproduced elongation (%) of the flashed ellipse as a function of its actual degree of elongation (%) in Experiment 1. The *y* axis indicates the percent elongation of the reproduced ellipse with respect to the actual elongation of the flashed ellipse; it is positive if the reproduced ellipse had the same direction of elongation as the flashed ellipse, zero if the reproduced ellipse was a circle, and negative if the reproduced ellipse was elongated perpendicular to the flashed ellipse. The error bars represent ±1 *SE*. The dashed line with a slope of 1 represents veridical perception. A linear relationship between the reproduced elongation and the actual elongation indicates that the observer reproduced the degree of elongation accurately to a constant scaling factor, namely, the slope of linear regression. A slope greater than 1 indicates overestimation (exaggeration) of the degree of elongation, and a slope less than 1 indicates underestimation. Note that all observers exaggerated the degree of elongation of the flashed ellipse. (b) The slopes as a function of the exposure duration of the ellipse. The thin curves are the data from the individual observers, and the thick curve is the mean.

r^2 = .995 for the mean (.985–.999 for the individual observers). This result thus verifies the reliability of the matching technique for the measurement of the perceived ellipticality of briefly flashed ellipses. It can also be seen in Figure 3a that all observers exaggerated the degree of elongation; the dashed line has a slope of 1, indicating the veridical degree of elongation.

The highly linear relationship between the reproduced elongation and the actual elongation (see Figure 3a; $r^2 > .98$ for all observers) indicates that the degree of exaggeration (defined as the ratio of the reproduced degree of elongation to the actual degree of elongation) is nearly constant across the variously elongated ellipses presented; in that case, regression slopes (with the actual degree of elongation being the independent variable and the reproduced degree of elongation being the dependent variable) are a meaningful estimate of a constant degree of exaggeration of ellipticality. The slopes obtained for the individual observers ranged from 1.9 to 4.4 (M = 2.8), indicating that the flashed ellipses appeared to the 5 observers as much as 1.9–4.4 times as elongated as they really were.

We thought it would be interesting to see if the degree of

exaggeration depended systematically on the exposure duration. As above, we used the regression slopes as indicators of the degree of exaggeration. When the regression analyses were performed separately for each exposure duration for each observer, the linearity was reasonable but not as impressive as it was before; the r^2 varied from .91 to .999 across observers and exposure durations.

As shown in Figure 3b, the degree of exaggeration (as indexed by the regression slopes), depended critically on the exposure duration. The pattern of dependence was similar for all observers except for S.G., who had a higher overall level of exaggeration. Overall (see the thick curve representing the mean), the degree of exaggeration (or the slope) climbed rapidly to a peak value at the exposure duration of ~150 ms and then began to fall gradually. This temporal pattern, characterized by a rapid initial rising component, indicates that the exaggeration of elongation occurred rather rapidly during the process of perceptual and/or memory encoding, rather than during memory retention while the observer was engaged in the matching task. Furthermore, there was no significant correlation between the degree of exaggeration (the thin curves in Figure 3b) and the reproduction duration[6] across different exposure durations for any of the observers: Pearson's $r = .56$, $p < .2$ for A.B.; $r = .12$, $p < .8$ for C.H.; $r = .003$, $p < 1$ for M.C.; $r = -.03$, $p < 1$ for S.G.; and $r = .65$, $p < .2$ for S.S. This further supports the claim that the exaggeration occurred perceptually and was not a function of the length of the reproduction interval.

We performed a similar set of analyses on the perceived size (area) to see how it depended on the degree of elongation and the exposure duration. In Figure 4a is plotted the perceived size (computed as the ratio of the reproduced area to the actual area) as a function of the degree of elongation of the flashed ellipse. Although the absolute magnitude of the perceived size varied across observers, it stayed relatively constant as a function of the elongation of the flashed ellipse.

In Figure 4b, the perceived size is plotted as a function of the exposure duration. The size was underestimated during the first ~200 ms of exposure compared with the asymptotic value. This pattern was seen in all observers, whereas individual differences were in the absolute level. This finding is consistent with Lindermann's (1922/1955) observation that a briefly flashed circle appears to expand at the onset of its exposure, starting at a size smaller than the resting size (asymptotic size in our case). As mentioned earlier, however, none of our observers reported any expansive motion of the flashed ellipses.

Recall Lindermann's (1922/1955) further claim that the expansive motion of flashed ellipses always appears larger in the horizontal than in the vertical direction, causing apparent horizontal elongation (relative to the veridical shape). To see if there was any systematic bias toward seeing horizontal elongation in our paradigm, we plotted the reproduced degree of horizontal elongation (%) for the flashed circles (actual elongation = 0%) in Figure 5. Greater positive values indicate greater horizontal elongation, whereas greater negative values indicate greater vertical elongation. Consistent with Lindermann's observation, a flashed circle was perceived as a horizontally elongated ellipse more or less by all observers—the horizontal bias. For the purpose of the current study, the horizontal bias is treated as a baseline setting;[7] note that the bias can be quite large for some observers (M.C. and S.G. in Figure 5).

In the following experiments that used lines and circles (Experiments 2–8), we intended to measure the degree of the apparent elongation of the test circle in the direction perpendicular to the orientation of the priming line, above and beyond the horizontal bias. To that end, we always used an equal number of trials with the vertical and the horizontal priming lines, which would elongate the test circle in the horizontal and the vertical directions, respectively. By averaging the results over the two priming line orientations, we averaged out any horizontal bias. Furthermore, in order to make the error bars for each observer reflect the trial-to-trial fluctuations in the distortion effect above and beyond the variance that was due to the observer's baseline orientation anisotropy (the possibly different strengths of the distortion effects from the vertical and the horizontal priming lines as well as the horizontal bias), we removed the main effect of the orientation of the priming line before we

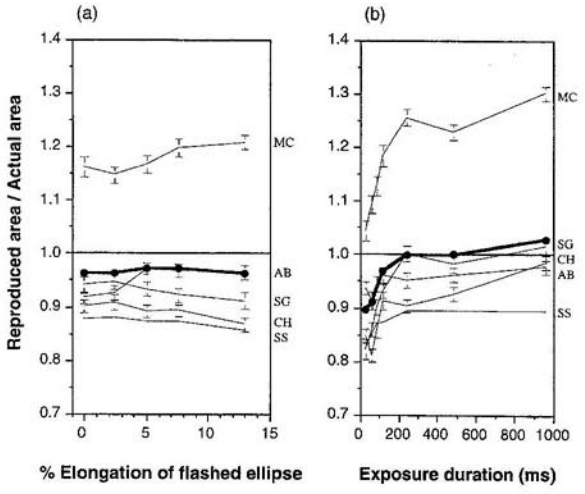

Figure 4. The reproduced area relative to the actual area of the flashed ellipse in Experiment 1 (a) as a function of the flashed ellipse's degree of elongation and (b) as a function of the ellipse's exposure duration. The thin curves are the data from the individual observers, and the thick curve is the mean. The error bars represent ±1 *SE*.

[6] The mean reproduction durations were 1,751 ms for A.B., 2,217 ms for C.H., 1,315 ms for M.C., 2,145 ms for S.G., and 4,441 ms for S.S.

[7] In Figure 3a, for example, we removed the horizontal bias by averaging the results over the vertical and the horizontal ellipses for each observer. The variance due to the bias was also removed from the error bars; we did this by removing the main effect of the ellipse orientation before computing the standard errors of the mean. Thus, the curves and the error bars shown in Figure 3a indicate how accurately the observers reproduced the relative degrees of elongation of the peripherally flashed ellipses.

computed the standard errors of the mean. Thus, the mean and the error bar data presented in Experiments 2–8 reflect the amount and the trial-to-trial fluctuation of the distortion effect above and beyond the possible effects of the baseline orientation anisotropy. A careful investigation of the orientation anisotropy is beyond the scope of this article.

In the last analysis we examined how the "structural noise" behaves as a function of the exposure duration. As discussed in the introduction, the structural noise manifests itself as random fluctuation of perceived shapes (degrees of elongation or aspect ratios in this case) from trial to trial. Here, the amount of fluctuation is computed as the standard deviation[8] of the reproduced degree of elongation (%). In Figure 6, the standard deviations (the thin curves for the individual observers and the thick curve showing the average across the observers) are plotted as a function of the duration of the stimulus presentation. Although the individual differences are salient, all observers exhibited a similar temporal pattern. It is easy to see that the amount of the trial-to-trial fluctuation of perceived elongation—that is, the structural noise—remained strong up to ~150 ms and then decreased rapidly with increasing exposure duration. The noise in the perceived size (computed as the standard deviation of [reproduced area]/[actual area]) behaved similarly as a function of the exposure duration, but the average drop in magnitude was small (~15%) compared with that for the structural noise (~40%; see Figure 6).

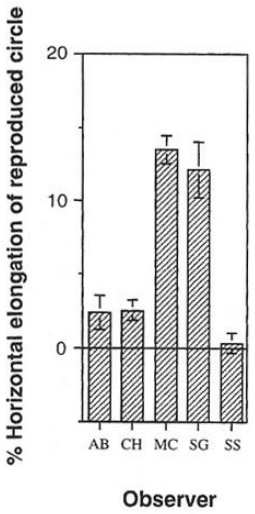

Figure 5. Flashed circles appear elongated horizontally—the horizontal bias (Experiment 1). The *y* axis indicates the degree of elongation (%) of the reproduced ellipse in the horizontal direction in response to a flashed circle; it is positive if the reproduced ellipse was horizontally elongated, zero if a circle was correctly reproduced, and negative if the reproduced ellipse was vertically elongated. Note that most observers tended to reproduce a flashed circle as a horizontally elongated ellipse. The data are collapsed over different exposure durations (30–1,000 ms). The error bars represent ±1 *SE*.

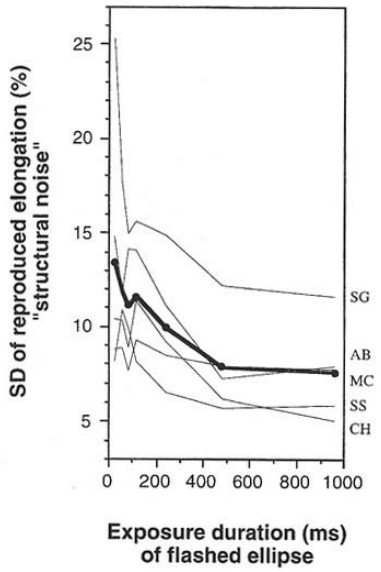

Figure 6. The standard deviation of the reproduced elongation (%) without the variances due to the horizontal bias and the perceptual exaggeration—that is, the "structural noise" (see text for detail)—as a function of the exposure duration (Experiment 1). The data are collapsed over the different degrees of elongation of the flashed ellipse. The thin curves are the data from the individual observers, and the thick curve is the mean.

In summary, we validated our matching method by showing that the reproduced and the actual degrees of elongation were linearly correlated, $r^2 = .995$. We also found that the observers always exaggerated the degree of elongation, seeing the flashed ellipses as more elongated than they really were. It is interesting to note that consistent exaggeration such as that shown in Figure 3a may increase observers' ability to discriminate among ellipses that are subtly different from a circle. The discrimination sensitivity as measured in d' would be a monotonically increasing function of the slope shown in Figure 3a unless the standard deviation also increased in proportion to the slope. At this point, we are agnostic about how far the degree of exaggeration (the slopes in Figure 3a) will remain relatively constant for larger degrees of elongation (for more obvious ellipses).[9]

[8] In order to reveal the "structural noise" component of the variance, we removed those variances that were due to the horizontal bias and the perceptual exaggeration (which varied systematically as a function of the exposure duration, as shown in Figure 3b). We accomplished this by removing the main effects of the orientation and the degree of elongation of the flashed ellipse before computing the standard deviation of the reproduced degree of elongation (%) for each exposure duration for each observer.

[9] The data from S.G. in Figure 3a show a hint of bowing down for larger degrees of elongation (i.e., a reduced degree of exaggeration for narrower ellipses).

The exaggeration grew rapidly with increases in the exposure duration, peaked at ~150 ms, and then began to fall very gradually. The rapid temporal growth confined to the initial ~150 ms indicates that the exaggeration process occurs rapidly during perceptual and/or memory encoding, but not during memory retention while the observer is doing the matching task—perceptual exaggeration. It will be interesting to see if the degree of exaggeration eventually goes to zero with a much longer exposure duration. The matched size also grows in the first ~200 ms of the stimulus onset and plateaus thereafter.

The structural noise, measured as the standard deviation (see Footnote 8) of the reproduced degrees of elongation, stayed high up to ~150 ms and then decreased rapidly with increasing exposure duration, falling substantially by ~300 ms (see Figure 6). Because the mask does not appear to overlap the preceding stimulus beyond ~50 ms of SOA (e.g., Eriksen & Hoffman, 1963; Georgeson, 1988; Georgeson & Georgeson, 1987; Turvey, 1973) and because the perceived clarity (which is inversely related to the neural noise of the lower level units with retinally localized receptive fields) seems to be already at its peak within ~200 ms (e.g., Rolls et al., 1994), our result seems to indicate that window of exposure duration (about 100–300 ms) exists in which the structural noise, which manifests itself as the variability in perceived shape rather than as degradations in image quality, is the dominant component in the variability of the visual percept. We speculate that the spontaneous neural noise of the high-level shape-tuned units (perhaps in IT) may underlie the structural noise.

Once our matching method was validated, we conducted a series of experiments in which we used briefly flashed lines and circles to examine the spatial and temporal characteristics of the shape distortion effects. Experiment 2 demonstrates the basic distortion effect and evaluates the classical explanations for it that are based on shape-changing apparent motion and a size aftereffect.

Experiment 2: The Basic Line-on-Circle Distortion Effect

The basic phenomenon is that when a flashed line just precedes a circle briefly flashed in the overlapping location, the circle appears to be elongated in the direction perpendicular to the orientation of the line. We have been calling the inducer of this distortion effect the *priming line* and the distorted figure the *test circle.* As discussed in the introduction, this phenomenon was first observed by Hartmann (1923/1955), who used a line longer than the diameter of the circle, as illustrated in Figure 1. He proposed that the distortion effect is created by the salient contractile motion of the line terminators and by the motion of the portion of the line inside the circle expanding into the circle—the motion-extrapolation hypothesis. When the line is longer than the diameter of the circle and the two stimuli are presented at the same location, not only could the distortion effect be due to the perceived motion of the line deforming into the circle, but it could also result from a size aftereffect occurring simultaneously in two orthogonal orientations, one along and the other perpendicular to the length of the line. Simultaneous adaptations to a lower overall spatial frequency along the length and a higher overall spatial frequency along the width of the priming line[10] could make the subsequently presented test circle appear shortened and elongated along the respective dimensions of the line—the size-aftereffect hypothesis. For example, Frome, Levinson, Danielson, and Clavadetscher (1979) showed that an adaptation to a vertical or horizontal grating makes a subsequently viewed rectangle elongated in the direction orthogonal to the bars of the grating.

In order to evaluate these two hypotheses, we varied the length of the priming line. The motion-extrapolation hypothesis predicts that the squashing effect should be considerably reduced when the line is made short enough to fall completely inside the circle because then the motion extrapolation of the line terminators should reverse to be expansive, counteracting the squashing effect. The perceived size should also increase because the motion extrapolation then would be totally expansive. The size-aftereffect hypothesis makes a similar prediction. Given that the size aftereffect along the direction of the line increases in proportion to the size contrast (line length relative to circle diameter), the squashing effect should increase while the perceived size of the test circle should decrease as the length of the priming line is increased. This prediction is expected to hold especially when the line length is increased from shorter than to longer than the diameter of the circle because the size contrast will reverse its polarity in the process.

Method

Observers. Six observers participated in the experiment.

Stimuli. The diameter of the test circle was 3.8°. The length of the priming line was varied from 0.5 to 2.5 times the diameter. The stimulus eccentricity was 6.5° at the center. Also see the General Method section.

Procedure. A vertical or horizontal priming line of a variable length was flashed for 30 ms randomly in the middle of one of the quadrants. After a fixed SOA of 180 ms, the test circle was presented for 60 ms at the location overlapping the priming line and was followed immediately by the random-dot mask, which lasted 255 ms (see Figure 2). The observer reproduced the perceived shape of the distorted test circle (as a horizontally or vertically elongated ellipse whose degree of elongation indicated the strength of the distortion effect) at the end of each trial (see the General Method section for details).

Each observer was given 160 trials: (4 repetitions) × (2 priming line orientations) × (5 line lengths) × (4 quadrants). The order of the trials was randomized for each observer. A short break was given after 80 trials.

Results and Discussion

Figure 7a shows the distortion effect (percent elongation of the reproduced test circle in the direction perpendicular to the priming line) as a function of the length of the priming line. A larger positive value indicates a larger distortion

[10] Note that lower spatial frequencies roughly correspond to larger sizes, and higher spatial frequencies to smaller sizes.

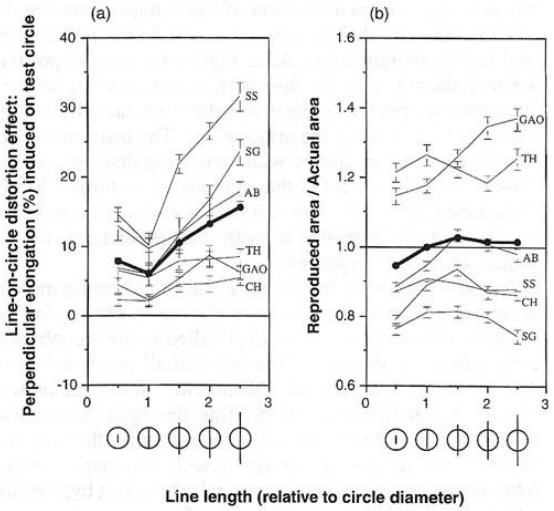

Figure 7. The shape distortion effect (line-on-circle) as a function of the length of the priming line in Experiment 2. (a) The reproduced elongation (%) of the test circle. The *y* axis indicates the percent elongation of the reproduced ellipse with respect to the orientation of the priming line; it is positive if the reproduced ellipse was elongated perpendicular to the priming line, zero if the reproduced ellipse was a circle, and negative if the reproduced ellipse had the same direction of elongation as the priming line. Thus, positive values indicate the expected distortion effect (shape contrast), zero indicates no effect, and negative values indicate an unexpected distortion effect (shape assimilation). This *y*-axis convention is also used in subsequent figures that show the line-on-circle distortion effects (i.e., Figures 10, 11, and 13–17). (b) The reproduced area relative to the actual area of the test circle. A value greater than 1 indicates that the reproduced area was greater than the actual area of the flashed circle, and vice versa. The length of the priming line relative to the test circle is depicted along the abscissa in both panels. The thin curves are the data from the individual observers, and the thick curve is the mean. The error bars represent ± 1 *SE*.

effect; a value of zero indicates no effect; and negative values indicate elongations of the test circle along the priming line. The thin curves are the data from the individual observers, and the thick curve is the mean. The distortion effect grew as the priming line was made 1–2.5 times as long as the diameter of the test circle. Surprisingly, however, the effect did not drop—it even slightly rebounded—as the priming line was reduced from equal to half the diameter of the test circle (so that the line was completely within the circle); the rebound was seen in all observers, $F(5, 1) = 7.50$, $p < .05$. This result contradicts both the motion-extrapolation and the size-aftereffect hypotheses. The former predicted a dramatic drop in the distortion effect as the motion from the line terminators to the circle was reversed to be expansive. The latter predicted a monotonic drop in the effect as the line was made shorter.

Figure 7b shows the perceived size of the test circle (the ratio of the matched area to the actual area) as a function of the length of the priming line. The perceived size depended little on the length of the priming line. This result provides further evidence against the two hypotheses. The motion-extrapolation hypothesis predicted that the expansive motion extrapolation of the line terminators would increase the apparent size of the test circle when the line was made short enough to be completely within the circle. The size-aftereffect hypothesis predicted that the test circle would appear smaller as the line was made longer because of the increased size contrast. Contrary to these predictions, Figure 7b shows that, if anything, the test circle appeared larger as the priming line was made longer.

An alternative explanation of these results is that the distortion effect is due to "shape contrast" between a line and a circle. The stronger effects obtained with longer priming lines could be due to the "linearness" of the priming shape being perceived more strongly for longer lines. It is reasonable to expect a shape-based priming to be stronger when the priming shape is more distinctive. Furthermore, the priming line length should not affect the apparent size of the test circle if the effect is due to pure shape contrast. The critical prediction of the shape-contrast hypothesis, however, is that the distortion effect should be independent of image interactions in the retinal space. In other words, if shape contrast is the underlying mechanism of the observed distortion effect, the effect should be fairly independent of spatial parameters such as distance and location. In the next experiment we evaluated this critical prediction.

Experiment 3: Is the Line–Circle Distortion Effect Independent of Location and Orientation?

In this experiment, the distance between the priming line and the test circle was varied from 0° up to 12° (over three times the diameter of the test circle) in horizontal and vertical directions. This manipulation, combined with the two priming-line orientations (vertical and horizontal), resulted in the generation of three distinct spatial configurations of the priming line and the test circle: overlapping (see Figure 8a), flanking (see Figure 8b), and radial (see Figure 8c).

In classic figural aftereffects, adapting contours repel test contours presented near them. In the case of a line contour, the figural aftereffect should be predominantly perpendicular to the line (see Figure 8). The figural-aftereffect hypothesis thus predicts different patterns of distortion for the three spatial configurations. In the overlapping configuration, the test circle should appear elongated perpendicular to the priming line (see Figure 8a). However, when the priming line is moved out of the test circle to a flanking position, the local repulsion effect should then push the neighboring contour laterally to make the test circle appear elongated *along* the line (see Figure 8b). When the priming line is positioned such that the line is pointing at the circle (the radial configuration), the contour repulsion should then hardly distort the test circle, except for a possible dent near the line terminator (see Figure 8c). The shape-contrast hypothesis, however, predicts an equivalent elongation perpendicular to the priming line for all three configurations. A pure shape interaction, by definition, should not depend on

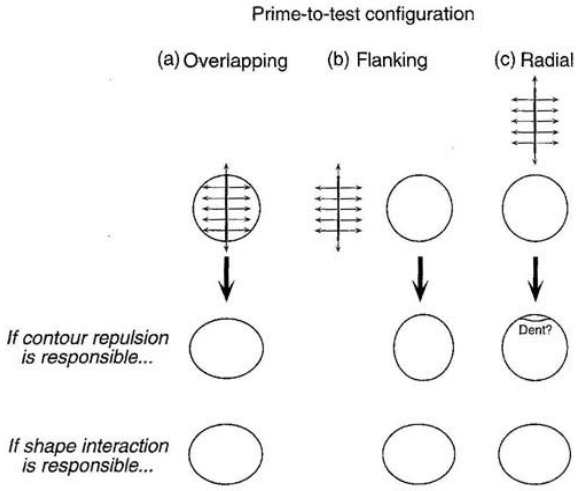

Figure 8. Predicted distortion effects for three distinct configurations of the priming line and the test circle in Experiment 3: (a) overlapping, (b) flanking, and (c) radial. A local-contour-repulsion hypothesis and the shape-contrast hypothesis make qualitatively different predictions for the flanking and the radial configurations.

the retinal coordinates of the interacting shapes. A shape-contrast effect should also occur across large distances, in contrast to figural aftereffects, which decay sharply with distance, the optimum distance ranging from 8′ to 3°, as reported in 13 studies (e.g., Fox, 1951; Kohler & Wallach, 1944; Sagara & Ohyama, 1957).

Method

Observers. Four observers participated in the experiment.

Stimuli. A test circle (3.8° in diameter) was presented for 60 ms in the middle of a randomly chosen quadrant at an eccentricity of 6.5° (to the center of the stimulus). Prior to presentation of the test circle, a vertically or horizontally oriented priming line (3.7° long) was flashed for 30 ms at a variable distance (0°–12°) horizontally or vertically away from the test circle (center to center). Because of the constraint of the monitor size, the distance was always measured toward one of the two adjacent quadrants. For example, if a test circle was to be presented in the upper left quadrant, a priming line would be flashed 0°–12° away from that location toward either the upper right or the lower left quadrant. Figure 9 shows all possible priming lines for a test circle presented in the upper left quadrant. Also see the General Method section.

Procedure. The trial events were identical to those in the previous experiment (see Figure 2) except that the priming line was flashed at various distances from the test circle and was always the same length. Each observer was given eight blocks of 64 trials ([2 priming line orientations] × [4 vertical + 4 horizontal distances] × [4 quadrants]), for a total of 512 trials. The order of the trials was randomized for each block for each observer. A short break was given at the end of each block.

Results and Discussion

Figure 10 shows the distortion effect (percent elongation of the reproduced test circle in the direction perpendicular to the priming line) as a function of the distance between the priming line and the test circle, collapsed over the flanking and radial configurations. As in Figure 7a, a larger positive value indicates a larger distortion effect, a value of zero indicates no effect, and negative values indicate elongations of the test circle along the priming line. The distortion effect decreased rather gradually with increasing distance, but for observers A.B. and S.G., the amounts of distortion hardly diminished up to 12°. This insensitivity to a large variation in distance is inconsistent with the predictions of the figural-aftereffect hypothesis.

We next looked at the flanking and radial configurations separately. Figure 11 shows the distortion effects for the flanking (open circles) and radial (filled circles) configurations (shown in Figure 8). The fact that all points in Figure 11 are positive indicates that the direction of elongation was always perpendicular to the priming line regardless of the prime-to-test distance or the configuration (flanking vs. radial). This finding is consistent with the shape-contrast hypothesis and contradicts the figural-aftereffect hypothesis, which predicted that the direction of apparent elongation would be along the priming line when the line was moved from the overlapping position to the flanking position (see Figures 8a and 8b).

Even though the direction of the distortion effect did not depend on spatial parameters, the magnitude of the effect clearly diminished faster for the radial configuration than for the flanking configuration, with increasing distance (see Figure 11). Although we do not know the origin of this quantitative effect of spatial configuration at this point, we

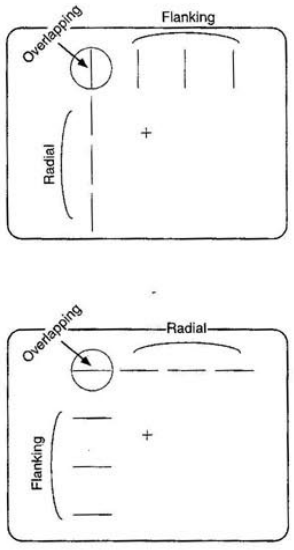

Figure 9. All possible priming lines in Experiment 3 are shown for a test circle flashed in the upper left quadrant. Reflecting the whole patterns about the horizontal meridian, the vertical meridian, and both meridia will give the priming lines for a test circle flashed in the lower left, upper right, and lower right quadrants, respectively.

show later (in Experiments 9 and 10) that the magnitudes of the shape-contrast effects obtained for the other two pairs of shapes we tested depended little on similar manipulations of the relative orientations of the interacting stimuli. Perhaps the particular orientation anisotropy observed with the priming lines is particular to linear stimuli that are known to be extensively coded at the early retinotopic stages of visual processing.

In the next experiment, we considered the hypothesis that perception of apparent motion from the priming stimulus to the test stimulus might be necessary for the distortion effect to occur. Although we presented an indirect piece of evidence in Experiment 2 that motion extrapolation could not explain the observed pattern of dependence of the distortion effect on the length of the priming line, we have not yet directly compared a motion-present condition with a motion-absent condition to see if perception of motion is in any way necessary for the distortion effect.

Experiment 4: Is Perception of Apparent Motion Necessary to See the Distortion Effect?

If a visual stimulus is flashed twice in succession across a spatial gap, various degrees of motion are perceived depending on spatial and temporal parameters such as interstimulus distance and SOA (e.g., Burt & Sperling, 1981; Cavanagh & Mather, 1989; Korte, 1915). This phenomenon has been described as *apparent motion.* It has also been shown that

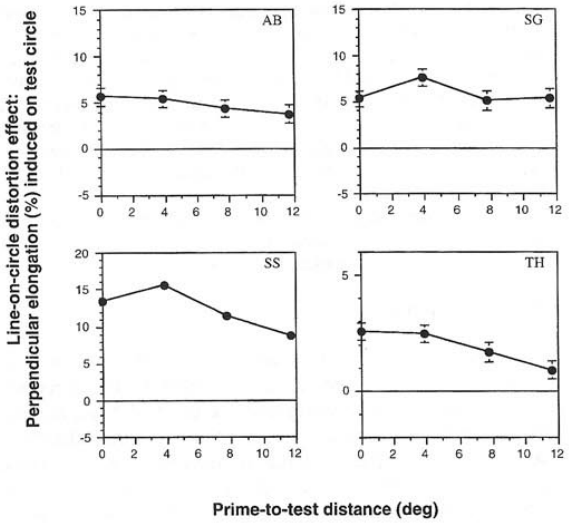

Figure 10. The shape distortion effect (line-on-circle) as a function of the distance between the priming line and the test circle in Experiment 3. As in Figure 7a, positive values indicate the degrees of elongation (%) of the reproduced test circle in the direction perpendicular to the priming line. The data are collapsed over the flanking and the radial priming lines. The error bars represent ±1 *SE.* Absence of an error bar indicates that the error bar is shorter than the marker symbol.

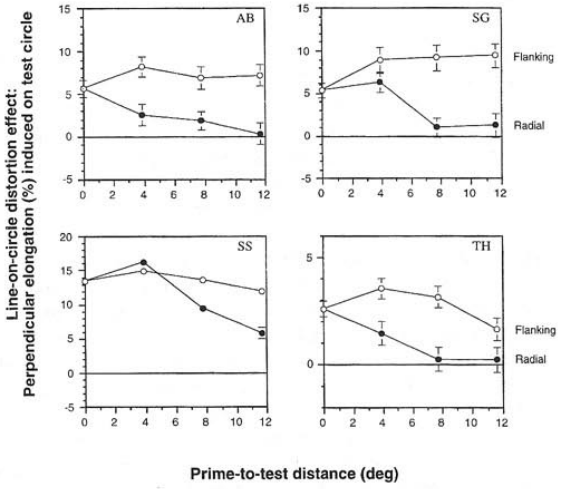

Figure 11. The same data shown in Figure 10 (Experiment 3) have been replotted to show the effects of the flanking (open circles) and the radial (filled circles) priming lines separately. Positive values indicate the degrees of elongation (%) of the reproduced test circle in the direction perpendicular to the priming line. The error bars represent ±1 *SE.* Absence of an error bar indicates that the error bar is shorter than the marker symbol.

when the shape of the stimulus changes between its successive presentations, the first shape appears to gradually transform to the second shape (e.g., Hartmann, 1923/1955; Helson, 1925; Kolers, 1972; Lindermann, 1922/1955).

Several studies have shown that the changes that occur during apparent motion overshoot the location and the shape of the "last motion token." The stimulus flashed last in a multistep apparent motion display sometimes appears as if the motion and the shape transformation continued in the mental representation slightly beyond the disappearance of the stimulus. This phenomenon has been called *representational momentum.* The amount of this nonveridical displacement has been shown to increase in proportion to the speed of apparent motion (Finke & Shyi, 1988; Freyd & Johnson, 1987; see also Nijhawan, 1994, for continuous motion) and to the delay in response following the disappearance of the last motion token (Freyd & Johnson, 1987); representational momentum thus acts much like physical momentum. A representational momentum effect has also been reported with multiple moving stimuli (Finke & Shyi, 1988). In that case, the last location of each moving stimulus appears nonveridically ahead in the direction of its own motion trajectory.

More relevant to our current discussion are the representational momentum effects in which apparent motion sequences involve changes in shape. Kelly and Freyd (1987) found that an expansive/contractile sequence of apparent motion (with no change in location) made the last motion token appear nonveridically larger/smaller, which is consistent with a momentum account. However, in the same study they found no momentum for changes in aspect ratio. In a

sequence of shape-changing apparent motion in which a narrow vertical rectangle transformed into a square (also with no change in location), the last square was seen veridically. This last finding suggests that our line-on-circle distortion effect, which would be an extrapolation of a change in aspect ratio, is not likely due to a mechanism underlying representational momentum effects.

Nevertheless, the line-on-circle distortion effect might still be contingent on perceiving apparent motion from the priming line to the test circle. In order to test this possibility directly, we generated a condition in which motion was not perceived between the priming line and the test circle. We accomplished this by making the priming line move smoothly away from the test circle in the "motion" trials. In an experimental session, the motion trials were randomly intermixed with the "flash" trials, in which the priming line was simply flashed as in Experiments 2 and 3. If the distortion effect is wholly motion contingent, little effect should be obtained in the motion trials. If apparent motion partially contributes to the distortion effect, the effect should be somewhat reduced in the motion trials. Finally, if the distortion effect is not due to perception of apparent motion at all, the effect in the motion trials should be just as strong as that in the flash trials.

Method

Observers. Nine observers participated in the experiment.

Stimuli and procedure. Because the goal of this experiment was to assess the contribution (if any) of the apparent motion between the priming line and the test circle to the distortion effect, the stimulus display was somewhat simplified compared with that in the preceding experiment. First, only the flanking condition was tested (see Figure 9). Second, the test circle (3.4° in diameter) was presented for 60 ms in the middle of either of the two upper quadrants (instead of all quadrants) at an eccentricity of 5.8° (to the center of the circle). Prior to presentation of the test circle, a vertically or horizontally oriented priming line (3.4° long) was always presented 4.1° away from the test circle (center to center). In order to increase the salience of the continuous motion of the priming line in the motion trials, the priming line was always presented nearer the fixation point than the test circle. In other words, a horizontal priming line was always presented below the test circle, and a vertical priming line was always displaced toward the vertical meridian relative to the test circle.

The priming line was made thicker (7.2′ wide compared with 2.7′ wide in the previous experiments) so that its smooth motion could be seen strongly in the motion trials. The priming line was always moved in the direction perpendicular to its orientation and away from the test circle. In a motion trial, the priming line was first presented for 90 ms at a location 7.2′ (the width of the line) closer to the test circle than in a corresponding flash trial; then the first line was erased and the second line was presented for 90 ms (with no temporal gap) at the adjacent location, in the direction away from the test circle and right where it would be flashed in a flash trial. The second line was then erased and the third line was presented (again with no temporal gap) another line-width farther from the test circle. The third line came on simultaneously with the test circle, stayed on for 60 ms, and was followed immediately by the random-dot mask, which lasted 255 ms (see Figure 12b).

A priming line in a motion trial thus moved smoothly away from the test circle in two steps of its width; the motion went symmetrically across the location where the priming line would be flashed in the corresponding flash trial. Because of the continuous motion of the priming line, no apparent motion was seen between the priming line and the test circle in a motion trial. In a flash trial, a priming line was flashed for 30 ms and the test circle was presented for 60 ms following an SOA of 180 ms; the random-dot mask (255 ms) immediately followed the test circle as in the previous experiment (see Figure 12a). Note that the SOA between the priming line and the test circle was the same (180 ms) in both the flash and the motion trials.

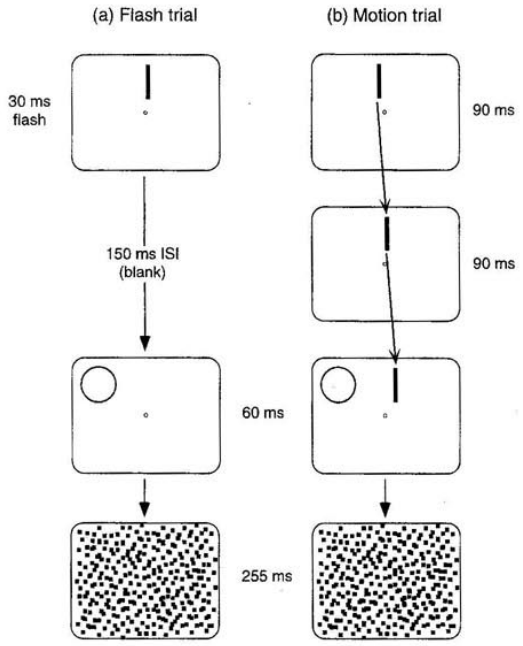

Figure 12. Trial events for Experiment 4: (a) flash trial and (b) motion trial. ISI = interstimulus interval.

Each observer was given 80 trials: (5 repetitions) × (2 priming line orientations) × (2 quadrants) × (2 conditions: flash and motion). The order of the trials was randomized for each observer.

Results and Discussion

Figure 13 shows the mean distortion effects (percent elongation of the reproduced test circle in the direction perpendicular to the priming line) for the flash trials and the motion trials. As before, a larger positive value indicates a larger distortion effect, a value of zero indicates no effect, and negative values indicate elongations of the test circle along the priming line. The distortion effects were significant (i.e., the degrees of reproduced elongation were significantly greater than zero) for the flash trials, $F(1, 8) = 10.98$, $p < .02$, and for the motion trials, $F(1, 8) = 13.63$, $p < .01$, indicating that the effect was not due to perception of apparent motion from the priming line to the test circle. Somewhat surprisingly, the effect was slightly, but significantly, larger in the motion trials than in the flash trials, $F(1, 8) = 11.44$, $p < .01$. This might have been due to

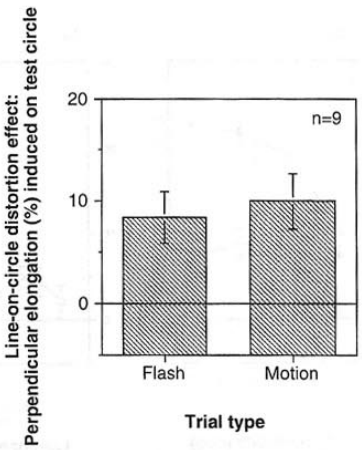

Figure 13. The shape distortion effect (line-on-circle) in the flash trials and the motion trials in Experiment 4. In the motion trials, the priming line moved smoothly so that no apparent motion was seen from the priming line to the test circle. Positive values indicate the degrees of elongation (%) of the reproduced test circle in the direction perpendicular to the priming line. The error bars represent ±1 *SE* for 9 observers.

stronger encoding of the priming line in the motion trials; possible factors include (a) the longer exposure duration of the priming line and (b) the priming line's attracting more attention because of its motion. Although these possibilities may be worthy of future study, this result appears to be unique to the distortion effect of a line on a circle. The magnitudes of the distortion effects did not differ between the motion trials and the flash trials in the later experiments where the other two pairs of shapes were tested (Experiments 9 and 10).

In the next four experiments, we further examined the temporal and spatiotemporal characteristics of the line-on-circle distortion effect. We varied the exposure duration of the test circle in Experiment 5 to determine how brief an exposure would be brief enough to see the distortion effect. In Experiment 6, we manipulated stimulus eccentricity and luminance contrast to see if the distortion effect generally increased with less signal available from the test circle. In Experiments 7 and 8 we varied the SOA between the priming line and the test circle to examine the storage time of the distortion effect both at the primed location (in Experiment 7) and across distance (in Experiment 8).

Experiment 5: How Brief a Test Exposure Is Brief Enough to See the Distortion Effect?

It is obvious that if a test circle is exposed for a long enough time, the distortion effect from a mere 30-ms flash of a line should eventually disappear. In this experiment, we measured how the effect diminished as a function of the test duration.

Method

Observers. Four observers participated in the experiment.

Stimuli. The stimuli used and their eccentricity (6.5° at the center) were the same as those used in Experiment 2 except that the length of the priming line was fixed at 7.3° (about twice as long as the diameter of the test circle). The priming line and the test circle were presented in any of the four quadrants, but they were presented at overlapping locations.

Procedure. The trial events were identical to those in Experiment 2 except that the exposure duration of the test circle was varied from 30 to 1,000 ms across trials (see Figure 2). Each observer was given 224 trials: (4 repetitions) × (2 priming line orientations) × (7 test circle durations) × (4 quadrants). The order of the trials was randomized for each observer. A short break was given roughly every 60 trials.

Results and Discussion

Figure 14 shows the distortion effect (percent elongation of the reproduced test circle in the direction perpendicular to the priming line) as a function of the exposure duration of the test circle. For all observers, the distortion effect fell

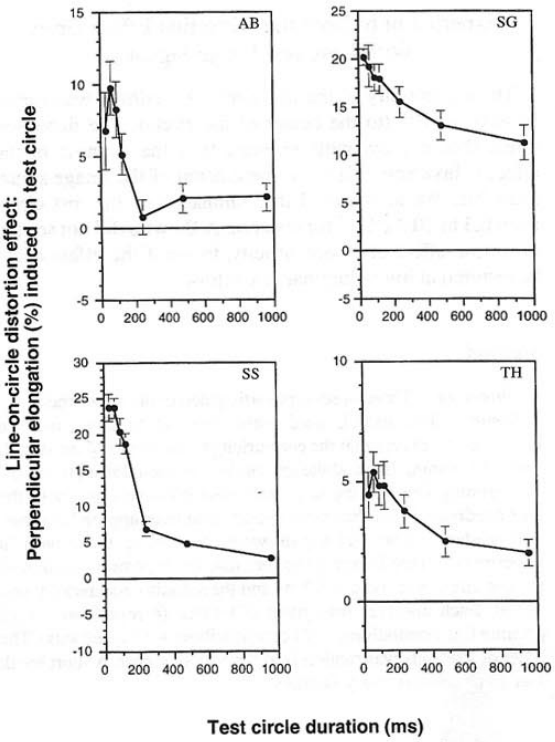

Figure 14. The shape distortion effect (line-on-circle) as a function of the exposure duration of the test circle in Experiment 5. Positive values indicate the degrees of elongation (%) of the reproduced test circle in the direction perpendicular to the priming line. The error bars represent ±1 *SE*. Absence of an error bar indicates that the error bar is shorter than the marker symbol.

within 150–300 ms, halfway to the lowest value corresponding to the longest exposure duration (960 ms).

Why are stronger distortion effects obtained with briefer exposures of the test circle? Two general hypotheses were evaluated. One was that the distortion effect is transient and decays during the presentation of the circle—the decay hypothesis. This hypothesis predicts that the distortion effect should fall at an equivalent rate when the prime-to-test SOA instead of the test circle duration is increased. We tested this possibility in Experiment 7. The second hypothesis was that less distortion effect should be obtained with longer exposure of the test circle because more image signal will then be available to "correct" the distorted initial representations—the correction hypothesis. This hypothesis predicts that reduced signals in general should increase the distortion effect. An image signal can be reduced without changing exposure duration by increasing the stimulus eccentricity[11] or by lowering its luminance contrast. The correction hypothesis thus predicts that the distortion effect should grow with larger eccentricity and lower luminance (against a dark background) of the test circle. We tested this possibility in Experiment 6.

Experiment 6: Does the Distortion Effect Grow With Less Test Image Signal?

The eccentricity of the test circle (3.7 cd/m^2) was varied from 0° to 10° (to the center of the circle). The distortion effect should grow with eccentricity if the strength of the effect is inversely related to the amount of the image signal available. We also varied the luminance of the test circle from 0.3 to 10.3 cd/m^2 for observer A.B., who did not see the distortion effect at 0° eccentricity, to see if the effect could be restored at lower luminance contrast.

Method

Observers. Three observers participated in the experiment.

Stimuli. The stimuli used were identical to those used in Experiment 5 except that the eccentricity to the center of the stimuli (both the priming line and the test circle) was varied from 0° to 10°. The priming line and the test circle were presented in any of the four quadrants,[12] but they were presented at overlapping locations.

Procedure. The trial events were identical to those used in Experiment 5 (see Figure 2) except that the exposure duration of the test circle was fixed at 60 ms and the stimulus eccentricity was varied. Each observer was given 244 trials: (4 repetitions) × (2 priming line orientations) × (4 eccentricities) × (4 quadrants). The order of the trials was randomized for each observer. A short break was given roughly every 60 trials.

Results and Discussion

Figure 15a shows that the distortion effect (percent elongation of the reproduced test circle in the direction perpendicular to the priming line) largely increased with eccentricity for all observers. This result supports the correction hypothesis in that the effect is larger when less stimulus signal is available for a given exposure duration.[13]

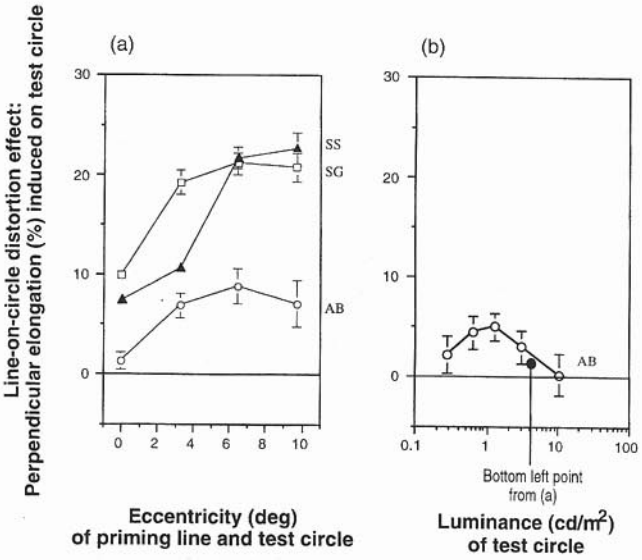

Figure 15. The shape distortion effect (line-on-circle) in Experiment 6 as a function of (a) stimulus eccentricity (3 observers) and (b) luminance (against a dark background) of the test circle at 0° eccentricity (for observer A.B.). Positive values indicate the degrees of elongation (%) of the reproduced test circle in the direction perpendicular to the priming line. The error bars represent ±1 *SE*. The filled circle in (b) corresponds to the bottom-left point in (a). Absence of an error bar indicates that the error bar is smaller than the marker symbol.

Note that the distortion effect almost vanishes at 0° eccentricity for A.B. We ran an additional test to see if the effect for A.B. could be raised substantially above zero at 0° eccentricity by reducing the luminance (against a dark background) of the test circle, that is, by reducing the signal. The priming line and the test circle were always presented at the center of the screen, and the luminance of the latter was varied from 0.3 to 10.3 cd/m^2. Observer A.B. was given 120 trials: (12 repetitions) × (2 priming line orientations) × (5 luminances). The order of the trials was randomized.

As shown in Figure 15b, A.B. did show significant effects (see the error bars) at 0° eccentricity when the luminance of

[11] The image sampling density falls off with increasing eccentricity because of the drop-off in the retinal photoreceptor cell density and the ganglion cell density and the consequent drop-off in the cortical magnification (e.g., Rijsdijk, Kroon, & van der Wildt, 1980; Wassle, Grunert, Rohrenbeck, & Boycott, 1990).

[12] The stimuli were centered at the fixation point when their eccentricity was zero.

[13] Because the eccentricity of the priming line and that of the test circle were varied in tandem, higher eccentricities weakened the signal of the priming line as well as that of the test circle. The result thus suggests that the weakening of the test signal has a stronger effect on the distortion effect than does the weakening of the priming signal. Further research is needed to determine how the magnitude of the distortion effect depends on the strength of the priming stimulus and the test stimulus separately.

the test circle was reduced. The effect peaked at about 1.25 cd/m^2. The falling of the effect at very low luminance values coincides with the similar falling of the distortion effect at the shortest exposure duration of the test circle (see A.B.'s data in Figure 14). This might be because too little stimulus signal was available for observers to reliably discriminate the elliptical shapes under these extreme conditions. We found in Experiment 1 (see Figure 3b) that perceptual exaggeration of a flashed ellipse also fell rapidly at very short exposure durations; this could also have contributed to the fall-off of the perceived distortion effect when too little signal was available.

In conclusion, the results from this experiment support the hypothesis that the distortion effects are weaker when more stimulus signal is available to "correct" the distorted initial representations of the test circle. In Experiment 7 we varied the SOA between the priming line and the test circle to see how the distortion effect decayed (or did not decay) over time during the SOA in the absence of a test presentation.

Experiment 7: Does the Distortion Effect Decay Over Time During the Prime-to-Test SOA?

Motion aftereffects have been known to decay much more slowly in the absence of a test presentation; this is known as the *storage effect* (e.g., Sekuler & Pantle, 1967; Spigel, 1962; Wohlgemuth, 1911). Similar storage phenomena have been reported in a contrast threshold elevation effect (Thompson & Movshon, 1978) and in figural aftereffects for adapt-to-test intervals up to tens of seconds depending on the duration of adaptation (e.g., Hammer, 1949; Ikeda & Obatani, 1953; Sagara & Ohyama, 1957). In Experiment 5, the distortion effect was shown to fall by half within 150–300 ms of the exposure of the test circle (see Figure 14). Because the SOA between the priming line and the test circle was 180 ms, the effect fell significantly within 330–480 ms after the onset of the priming line.

In the present experiment, the prime-to-test SOA was varied from 0 to 1,500 ms. On the one hand, if a temporal decay is responsible for the fall-off of the distortion effect with increasing test duration, the effect should fall substantially within 330–480 ms of the SOA even without a presentation of the test circle. On the other hand, if the fall-off is caused by the incoming signal from the test circle, as suggested by the results of Experiment 6, the effect should "store" over a much longer SOA.

Method

Observers. Four observers participated in the experiment.

Stimuli. The stimuli used and their eccentricity (6.5° at the center) were identical to those used in Experiment 2 except that the length of the priming line was fixed at 3.7° (comparable to the diameter of the test circle). The priming line and the test circle were presented in any of the four quadrants, but they were presented at overlapping locations.

Procedure. The trial events were identical to those in Experiment 2 except that the SOA between the priming line and the test circle was varied from 0 to 1,500 ms and the exposure duration of the test circle was fixed at 60 ms (see Figure 2). In the special case in which the SOA was zero, the priming line and the test circle were presented simultaneously for 60 ms.

Each observer was given two blocks of 208 trials ([2 repetitions] × [2 priming line orientations] × [13 SOAs] × [4 quadrants]), for a total of 416 trials. The order of the trials was randomized for each block for each observer. A short break was given approximately every 60 trials.

Results and Discussion

In Figure 16, the distortion effect is plotted as a function of the SOA between the priming line and the test circle. It took some build-up time (100–400 ms) for the effect to reach its maximum strength. The effect then remained undiminished for as long as 1,500 ms in the absence of a test presentation, whereas it fell considerably within 330–480 ms (180 ms of SOA plus 150–300 ms of exposure duration) in the presence of the test circle (see Figure 14). This result thus further supports the hypothesis that the rapid fall-off of the distortion effect is due to the visual system "correcting" the initially distorted representations by using the additional signals coming from a prolonged presentation of the test circle.

In Experiment 8 we repeated the present experiment except that we flashed the priming line 9.2° away from the test circle. Our aim was to see if the same degree of storage would be obtained across a large spatial gap.

Experiment 8: Is There Storage Across a Spatial Gap?

As in the previous experiment, we varied the SOA between the priming line and the test circle, but we always flashed the priming line 9.2° (2½ times the diameter of the test circle) away from the test circle to see if the long storage found with the overlapping configuration would also be found across a spatial gap.

Method

Observers. Four observers participated in the experiment.

Stimuli. The stimuli used were identical to those used in Experiment 7.

Procedure. The trial events were also identical to those in the previous experiment[14] (see Figure 2) except that the priming line was always flashed distant from the test circle. As in Experiment 3, because of the constraint of the monitor, the priming line was presented randomly across either the horizontal or the vertical meridian from the test circle (see Figure 9). Each observer was given two blocks of 208 trials ([2 priming line orientations] × [13 SOAs] × [4 quadrants] × [2 priming line locations per test circle]), for a total of 416 trials. The order of the trials was randomized for each block for each observer. A short break was given approximately every 60 trials.

Results and Discussion

The results are shown in Figure 17 (filled circles with black curves) along with the data from the previous experi-

[14] Because of a technical problem, the SOA = 0 condition was not tested in this experiment.

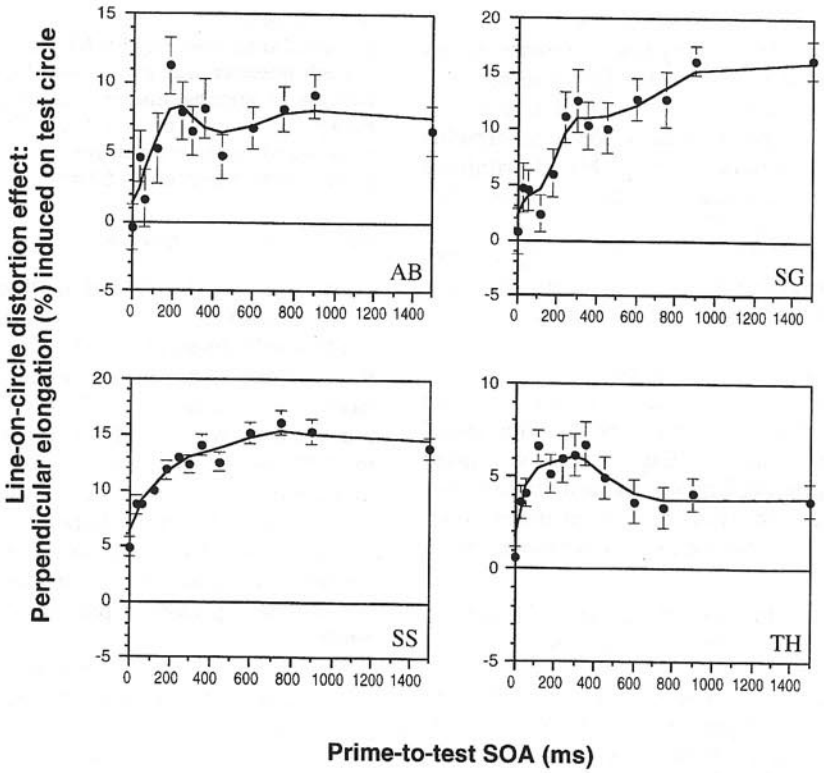

Figure 16. The shape distortion effect (line-on-circle) as a function of the stimulus onset asynchrony (SOA) between the priming line and the test circle when the two stimuli were presented at the overlapping location (Experiment 7). Positive values indicate the degrees of elongation (%) of the reproduced test circle in the direction perpendicular to the priming line. The smooth curves are the five-channel binomial fits. The error bars represent ±1 *SE*.

ment (open circles with gray curves) for comparison. The result of the comparison is rather surprising. The patterns for the two experiments are systematically different for all observers. The distortion effect across distance peaked faster and decayed considerably within ~400 ms in the absence of a test presentation. Note that it is not simply that the distortion effect had shorter persistence across distance, because that fact cannot explain why the effect rose faster across distance than at the overlapping location.

The results indicate that the shape interactions are relatively insensitive to the prime-to-test distance only if the prime-to-test SOA is within a narrow window of about 100–200 ms. The following factors may underlie the observed interaction between the distance and the SOA. First, low-level (local) contour effects as well as high-level shape effects are expected to contribute to the distortion effect when the priming line and the test circle are presented at the overlapping location. It is likely that the temporal characteristics are different between the low-level and high-level processes. The long storage might be a local phenomenon in that it occurs only at the location where the priming shape has been presented. It may also be possible that two shapes presented at the same location in very rapid succession may be processed by the same set of shape-tuned neurons that respond to the superimposed shapes (e.g., a ⓘ for the superimposed | and ○) rather than by those neurons that respond to each of the two separate shapes. This might explain the slow rising of the distortion effect in the same-location condition; for the two shapes to interact, they must be processed by different sets of shape-tuned neurons. Further research is needed to test these and other possibilities.

So far we have extensively examined the spatial and temporal characteristics of the interactions between a flashed line and a subsequently flashed circle. The results seem to indicate that the interactions are of shape contrast; that is, the distortion effect appears to occur across large distances in such a way that the test circle appears more dissimilar to the priming line (i.e., the test circle appears elongated in the direction orthogonal to the orientation of the priming line). So far, however, we have provided no evidence that this effect generalizes to shapes other than lines and circles. Thus, in the final two experiments, we tested two new pairs of shapes to see if they also exhibited the shape-contrast effect. The following criteria were used to choose the shapes to be tested. On the one hand, we wanted the defining characteristics of the priming shapes to be qualitatively different from and more complex than a line, which has only length and orientation. On the other hand, the nature of the distortions and the test shapes themselves needed

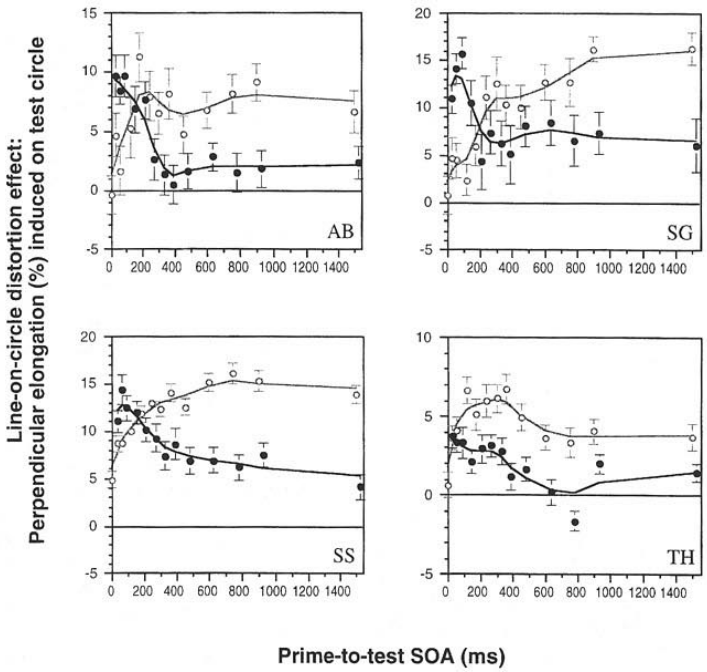

Figure 17. The shape distortion effect (line-on-circle) in Experiment 8 as a function of the stimulus onset asynchrony (SOA) between the priming line and the test circle when the prime-to-test distance was 9.2° (filled circles with black curve). The data from Experiment 7, in which the priming and the test stimuli were presented at the same location, are also shown (open circles with gray curve) for comparison. Positive values indicate the degrees of elongation (%) of the reproduced test circle in the direction perpendicular to the priming line. The smooth curves are the five-channel binomial fits. The error bars represent ±1 *SE*.

to be simple enough that the distortion could be discernible during a brief presentation of the test shape. The two pairs thus chosen were a triangle and a square (see Figure 18) and mouthlike shape with net curvature and a flattened diamond with no net curvature (see Figure 22); these pairs were tested for shape-contrast effects in Experiments 9 and 10, respectively.

Experiment 9: Does a Shape (Taper)-Contrast Effect Occur Between a Triangle and a Square?

The priming shape used was an isosceles triangle pointing to the left or the right, and the test shape was a square similar in size to the triangle (see Figure 18). The shape-contrast effect by definition should distort the test square in such a way that it appears more dissimilar to the preceding priming triangle. For example, a priming triangle pointing to the left is characterized by the asymmetry in size between its right and left ends, that is, by its tapering off to the left. So the shape-contrast effect in this case would induce the opposite tapering on the test square. In other words, the test square should be distorted into a trapezoid with its right side shorter than its left side. Similarly, a priming triangle pointing to the right should distort the test square into a trapezoid tapering off to the left. Note that the difference between the left-pointing and right-pointing triangles is present only at the level of the global shape; both triangles consist of an identical set of three line segments (see Figure 18). Thus, the sum of low-level orientation-specific interactions between the line segments composing the priming triangle and those composing the test square should produce no shape-contrast effect.

As noted earlier, if the distortion effect occurs at a shape processing level, the effect should be obtained across a spatial gap and be independent of the spatial configuration of the interacting shapes. Furthermore, as in Experiment 4, we intermixed the motion trials, in which the priming triangle was smoothly moved, with the flash trials, in which it was simply flashed, to see if perception of apparent motion between the priming and test stimuli made any contribution to the distortion effect in this case.

Method

Observers. Nine observers participated in the experiment.

Stimuli and procedure. The dimensions of the priming triangle and the test square are shown in Figure 18. As in Experiment 4, the priming triangle was drawn with thicker lines (7.2′) to increase the

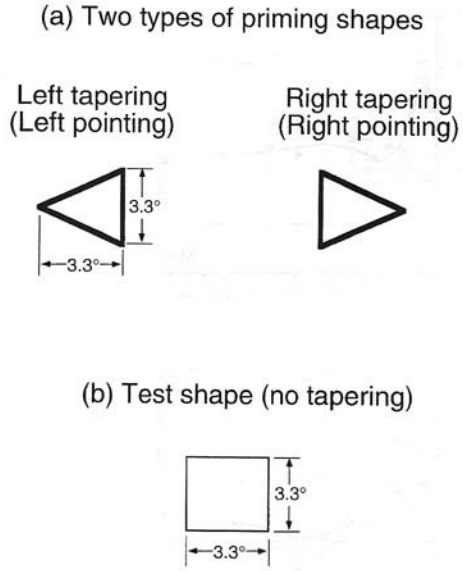

Figure 18. Stimuli used in Experiment 9 (taper-contrast experiment). (a) Two types of priming stimuli, left-pointing and right-pointing isosceles triangles. Note that the two priming stimuli, though pointing in opposite directions, are composed of the identical set of three line segments. (b) Symmetric test stimulus, a square.

salience of its motion in the motion trials. The test square was drawn with 2.4′ lines. Unlike in the previous experiments in which the test circle was flashed in a peripheral field (except in Experiment 6, in which the eccentricity of the test circle was varied), the test square was always presented centrally such that its center coincided with the fixation point. This modification was made because a pilot study showed that a peripherally flashed test square appeared "randomly" distorted from trial to trial, or perhaps distorted in a location-dependent manner yet to be uncovered, such that it was difficult to isolate the distortion effect that was due to the priming triangle. Central presentation substantially reduced the seemingly random distortions.

The priming triangle was pointing either to the left or to the right and was presented above, below, to the left of, or to the right of the test square at a distance of 6.1° (center to center). As shown in Figure 19, this generated two unique spatial configurations, that is, two unique orientations of the priming triangle and the test square relative to each other. In one configuration, the triangle pointed either toward or away from the test square—Configuration 1. This occurred when the triangle was presented either to the right or to the left of the test square. In the other configuration, the triangle pointed in the direction orthogonal to the virtual line connecting the centers of the two stimuli—Configuration 2. This occurred when the triangle was presented either above or below the test square.

In a motion trial, the priming triangle always moved backward; the one pointing to the left moved rightward, and the one pointing to the right moved leftward. The movement was thus toward or away from the test square in Configuration 1 and tangential to the test square in Configuration 2. The movement path was always symmetrical across the location where the priming triangle would be flashed in a corresponding flash trial. The triangle was first presented for 90 ms at 14.4′ to the left/right of the flash location; the first triangle was erased and the second triangle was presented for 90 ms (with no temporal gap) at the flash location. The second triangle was then erased and the third triangle was presented (again with no temporal gap) at 14.4′ to the right/left of the flash location. The third triangle came on simultaneously with the test square, stayed on for 60 ms, and was followed immediately by the random-dot mask, which lasted 255 ms (see Figure 20b). The motion thus generated appeared smooth. Because of the continuous motion of the priming triangle, no apparent motion was seen between the priming triangle and the test square in a motion trial.

In a flash trial, the priming triangle was flashed for 30 ms and the test square was presented for 60 ms following an SOA of 180 ms; the random-dot mask (255 ms) immediately followed the test square. Note that the SOA between the priming triangle and the test square was the same (180 ms) in both the flash and the motion trials (see Figure 20a).

We used a single-parameter matching method to approximate perceived distortions of the test square. The matching square identical to the test square was presented at the end of each trial following the mask. It was centered at the fixation point just like the test square. The observer distorted the matching square into a trapezoid tapering off to the right/left by moving the computer mouse laterally to the right/left. When the adjustment resulted in an acceptable approximation of the distorted test square, the observer clicked the mouse, and the lengths of the left and right sides of the

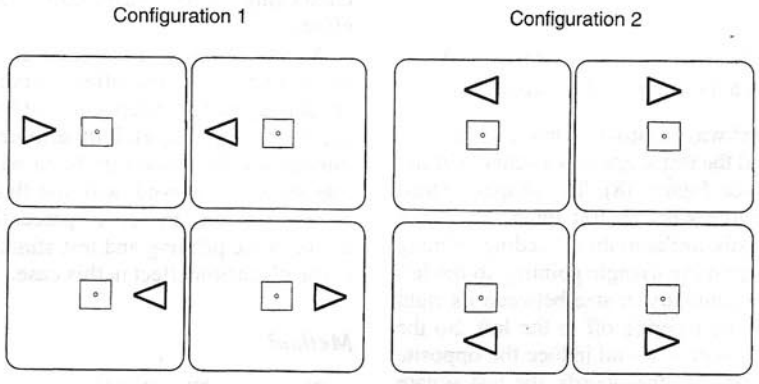

Figure 19. Two unique configurations of the priming triangle and the test square in Experiment 9. In Configuration 1, the priming triangle points toward or away from the test square. In Configuration 2, the priming triangle points in a direction tangential to the test square.

matched trapezoid were recorded. This particular method of reproduction was used because a pilot study showed that the dominant distortion of the test square was always one that made the test square appear to be a trapezoid tapering either slightly to the right or slightly to the left.

From the lengths of the left and right sides of the reproduced trapezoid, we computed an index of the degree of taper, "percent taper." We computed it by dividing the difference between the longer side and the shorter side by the shorter side and multiplying by 100: [(longer side) − (shorter side)]/(shorter side) × 100. The value indicates the degree of taper in terms of the percentage by which the longer side is longer than the shorter side. For example, a 0% taper would indicate a perfect square, whereas a 50% taper would indicate a trapezoid with a longer side 50% longer than its shorter side. For the purpose of measuring the shape (taper)-contrast effect, a positive sign was given if the reproduced trapezoid and the priming triangle were tapered on opposite sides; otherwise (i.e., if the reproduced trapezoid and the priming triangle were tapered on the same side), a negative sign was given. Thus, positive values of percent taper indicate a shape (taper)-contrast effect, 0% taper indicates no effect, and negative percentages indicate the test square appeared tapered in the same direction as the priming triangle.

Each observer was given 96 trials: (6 repetitions) × (2 priming triangle orientations: pointing to the right or the left) × (4 priming triangle locations: left, right, top, and bottom) × (2 conditions: flash and motion). The order of the trials was randomized for each observer.

Results and Discussion

Figure 21a shows the mean distortion effects for the flash and motion trials in terms of the percent taper discussed above. Significant shape (taper)-contrast effects were obtained (i.e., percent taper was significantly greater than zero) both in the flash trials, $F(1, 8) = 12.54$, $p < .01$, and in the motion trials, $F(1, 8) = 17.27$, $p < .005$. This result confirms the result of Experiment 4 which showed that the distortion effect was not due to perception of apparent motion from the priming shape to the test shape. However, unlike the distortion effect of a line on a circle, which was significantly stronger for the motion trials, the effect obtained here was equivalent for the flash and the motion trials, $F(1, 8) = 0.56$, $p < .5$.

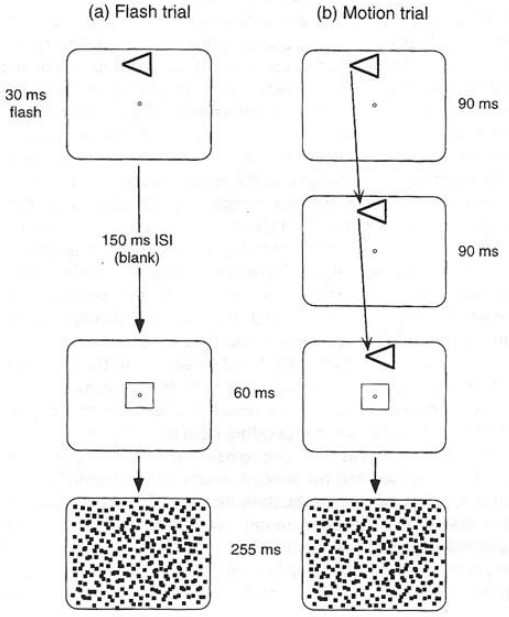

Figure 20. Trial events for Experiment 9: (a) flash trial and (b) motion trial. ISI = interstimulus interval.

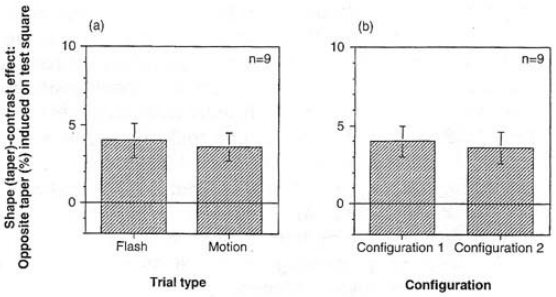

Figure 21. The taper-contrast effect in Experiment 9. The y axis shows the degree of taper (percent taper; see text) of the reproduced trapezoid relative to the direction of taper of the priming triangle; it is positive if the reproduced trapezoid and the priming triangle were tapered on opposite sides, zero if the reproduced trapezoid was a square, and negative if the reproduced trapezoid and the priming triangle were tapered on the same side. Thus, positive values indicate a taper-contrast effect, zero indicates no effect, and negative values indicate an unexpected "taper-assimilation" effect. (a) Comparison between the flash and the motion trials. In the motion trials, the priming triangle moved smoothly such that no apparent motion was seen from the priming triangle to the test square. The data are collapsed over the two configurations. (b) Comparison between Configurations 1 and 2 (refer to Figure 19). The data are collapsed over the trial types (flash and motion). Error bars represent ±1 *SE* for 9 observers.

In Figure 21b, the same data are replotted with respect to the spatial configuration of the priming triangle and the test square. Earlier we discussed that there are two unique configurations of the two shapes in terms of their orientations relative to each other: Configuration 1, in which the triangle points toward or away from the square, and Configuration 2, in which the triangle points tangentially to the square (see Figure 19). As can be seen in Figure 21b, the shape-contrast effect was obtained for both configurations: $F(1, 8) = 16.30$, $p < .005$ for Configuration 1, and $F(1, 8) = 13.08$, $p < .01$ for Configuration 2. Furthermore, unlike the line-on-circle distortion effect (see Figure 11), the magnitude of the triangle-on-square distortion effect did not depend on the spatial configuration, $F(1, 8) = 1.74$, $p < .3$.

For Configuration 1, one might argue that the triangles pointing toward the square (the leftmost column in Figure 19) may be qualitatively distinct from the triangles pointing away from the square (the other left column in Figure 19). We found no significant difference in the amount of the distortion effect between the pointing-toward and the point-

ing-away configurations for either the flash trials or the motion trials. For the flash trials, the mean percent taper values were 4.2 (SE = 1.2) for the pointing-toward configuration and 3.9 (SE = 1.3) for the pointing-away configuration, which did not differ significantly from each other, $F(1, 8) = 0.22$, $p < .7$. For the motion trials, the mean percent taper values were 3.9 (SE = 0.9) and 4.2 (SE = 0.9) for the two configurations, which also did not differ significantly from each other, $F(1, 8) = 0.59$, $p < .5$. These results suggest that the priming triangle and the test square interact at the level of processing in which shapes are coded independently of spatial parameters.

In the final experiment, we tested the other pair of shapes—namely, a mouthlike shape with upward or downward curvature and a flattened diamond with no net curvature—to see if they also interacted to produce a shape-contrast effect.

Experiment 10: Does a Shape-Contrast Effect Occur in the Dimension of Curvature?

The priming shape used was a mouthlike shape that curved upward or downward (see Figure 22a). The defining characteristic of the priming shape was its overall curvature: upward curving or downward curving. The test shape was a flattened diamond with vertical symmetry, that is, with no overall upward or downward curvature (see Figure 22b). The overall size of the test diamond was similar to that of the priming mouth. Because by definition the shape-contrast effect involves distortions of the test shape in the direction of increased figural dissimilarity to the priming shape, we expected that the priming mouth would induce the opposite curvature on the test diamond. In other words, if the priming mouth had upward/downward curvature, the test diamond would appear to have downward/upward curvature if a shape-contrast effect occurred between the two shapes. Note that, as in the previous experiment, the stimuli were designed such that the difference between the upward-curving and downward-curving mouths was present only at the level of global shape; both priming mouths consisted of an identical set of four line segments (see Figure 22). Thus, the sum of low-level orientation-specific interactions between the constituent line segments of the priming mouth and the test diamond should produce no shape-contrast effect.

As discussed earlier, if the distortion effect occurs at a shape processing level, the effect should be obtained across a spatial gap and be independent of the spatial configuration of the interacting shapes. Again, as in Experiments 4 and 9, we moved the priming shape smoothly in half of the trials (motion trials) to see if perception of apparent motion between the priming and test stimuli made any contribution to the distortion effect.

Method

Observers. Nine observers participated in the experiment.

Stimuli and procedure. The dimensions of the priming mouth and the test diamond are shown in Figure 22. As in Experiments 4 and 9, the priming mouth was drawn with thicker lines (7.2′) to increase the salience of its motion in the motion trials. The test diamond was drawn with 2.4′ lines. It was always presented centrally such that its center coincided with the fixation point; as in Experiment 9, we made this modification to reduce the seemingly random distortions on the test diamond that its peripheral presentation would entail.

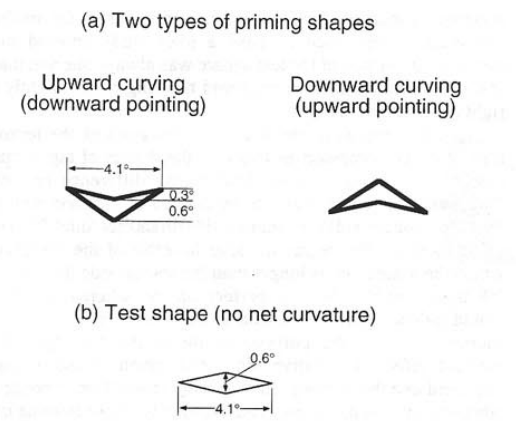

Figure 22. Stimuli used in Experiment 10 (curvature-contrast experiment). (a) Two types of priming stimuli, upward-curving (downward-pointing) and downward-curving (upward-pointing) "mouths." Note that the two priming stimuli, though opposite in net curvature, are composed of the identical set of four line segments. (b) Test shape, a flattened diamond with no net curvature.

The priming mouth was either upward curving or downward curving and was presented above, below, to the left of, or to the right of the test diamond at a distance of 4.5° (center to center). As shown in Figure 23, this generated two unique spatial configurations, that is, two unique orientations of the priming mouth and the test diamond relative to each other. In one configuration, the curvature of the mouth pointed either toward or away from the test diamond—Configuration 1. This occurred when the mouth was presented either above or below the test diamond. In the other configuration, the curvature of the mouth pointed in the direction orthogonal to the virtual line connecting the centers of the two stimuli—Configuration 2. This occurred when the mouth was presented either to the right or to the left of the test diamond.

In a motion trial, the priming mouth always moved backward, as did the priming triangle in Experiment 9; the upward-pointing mouth moved downward, and the downward-pointing mouth moved upward. The movement was thus toward or away from the test diamond in Configuration 1 and tangential to the test diamond in Configuration 2. As in Experiment 9, the movement path was always symmetrical across the location where the priming mouth would be flashed in a corresponding flash trial. The mouth was first presented for 90 ms at 14.4′ above/below the flash location; the first mouth was erased and the second mouth was presented for 90 ms (with no temporal gap) at the flash location. The second mouth was then erased and the third mouth was presented (again with no temporal gap) at 14.4′ below/above the flash location. The third mouth came on simultaneously with the test diamond, stayed on for 30 ms,[15] and was followed immediately by the random-dot mask,

[15] A shorter duration was used to enhance the distortion effect.

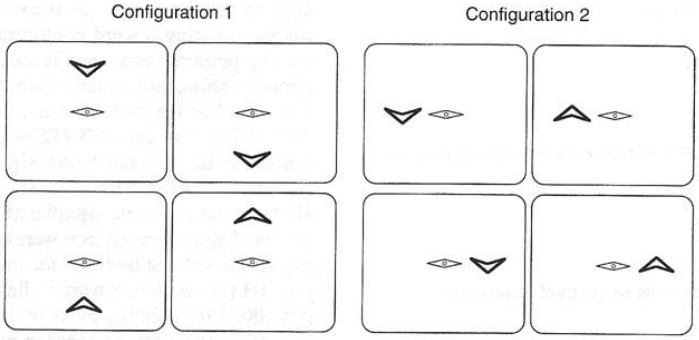

Figure 23. Two unique configurations of the priming mouth and the test diamond in Experiment 10. In Configuration 1, the curved priming mouth points toward or away from the flat test diamond. In Configuration 2, the priming mouth points in a direction tangential to the test diamond.

which lasted 255 ms (see Figure 24b). The motion thus generated appeared smooth. Because of the continuous motion of the priming mouth, no apparent motion was seen between the priming mouth and the test diamond in a motion trial.

In a flash trial, the priming mouth was flashed for 30 ms and the test diamond was presented for 30 ms following an SOA of 180 ms; the random-dot mask (255 ms) immediately followed the test diamond. Note that as in Experiment 9, the SOA between the priming mouth and the test diamond was the same (180 ms) in both the flash and the motion trials (see Figure 24a).

A two-alternative forced choice method instead of a matching method was used in this experiment. A pilot study showed that although the distortion effect in general appeared to be that of shape (curvature) contrast, the exact appearance of the distortion varied from trial to trial. Preceded by a downward-pointing mouth, the test diamond could appear distorted, for example, in any of the following ways: as an upward-pointing mouth (see Figure 25a), as a diamond with more acute curvature on the upper half (see Figure 25b), or as a diamond with the ends of its "wings" bent downward (see Figure 25c). Although all of these distortions are consistent with a shape-contrast effect in that the test diamond appears to point upward (having curvature opposite to that of the priming shape), it is difficult to reproduce this variety of distortions with a simple matching method. Thus, the observer in this experiment was told to make a two-alternative forced-choice response as to whether the overall shape of the test diamond appeared to be pointing upward or downward.

Each observer was given 96 trials: (6 repetitions) × (2 priming mouth curvatures: pointing upward or downward) × (4 priming mouth locations: left, right, top, and bottom) × (2 conditions: flash and motion). The order of the trials was randomized for each observer.

Results and Discussion

Figure 26a shows the mean distortion effects for the flash trials and the motion trials in terms of the percentage of the trials in which the responses were consistent with the shape-contrast effect, that is, the trials in which the observer reported the net curvature of the test shape to be opposite that of the priming shape. Thus, any values above 50% (chance) indicate a shape-contrast effect.

Significant shape-contrast effects were obtained (i.e., the values were significantly above 50%) both in the flash trials, $F(1, 8) = 41.04$, $p < .0005$, and in the motion trials,

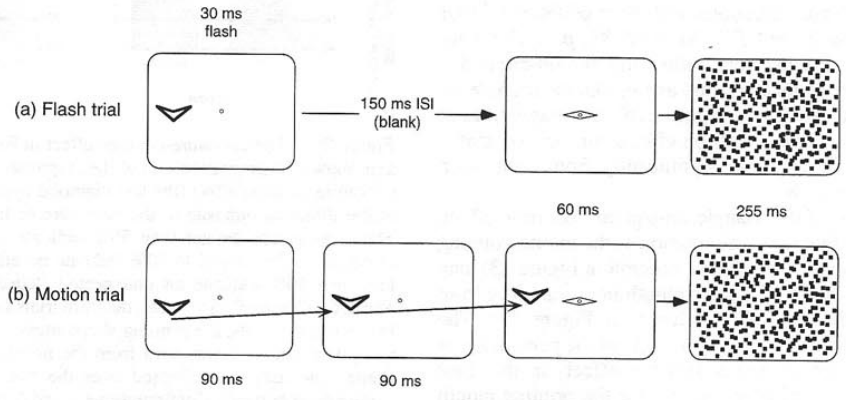

Figure 24. Trial events for Experiment 10: (a) flash trial and (b) motion trial. ISI = interstimulus interval.

(a) Upward-pointing mouth

(b) Diamond with more acute curvature on the upper half

(c) Diamond with ends of its wings bent downward

Figure 25. Representative examples of percepts of the distorted test diamond preceded by the downward-pointing priming mouth in Experiment 10: (a) upward-pointing mouth, (b) diamond with more acute curvature on the upper half, (c) diamond with ends of its "wings" bent downward. Because a two-alternative forced-choice method was used, the observer indicated the perceived net curvature of the test shape to be upward pointing for all of these observations.

$F(1, 8) = 66.39, p < .00005$. This result confirms the results of Experiments 4 and 9 that showed that the distortion effect was not due to perception of apparent motion from the priming shape to the test shape. Unlike the distortion effect of a line on a circle, but like that of a triangle on a square, the effect did not differ for the flash and the motion trials, $F(1, 7) = 0.87, p < .4$.

In Figure 26b, the same data are replotted with respect to the spatial configuration of the priming mouth and the test diamond. Earlier we noted that there are two unique configurations of the two interacting stimuli in terms of their orientations relative to each other: Configuration 1, in which the curvature of the mouth points toward or away from the diamond, and Configuration 2, in which the curvature of the mouth points tangentially to the diamond (see Figure 23). As can be seen in Figure 26b, the shape-contrast effect was obtained for both configurations: $F(1, 8) = 60.04, p < .0001$ for Configuration 1, and $F(1, 8) = 47.81, p < .0005$ for Configuration 2. Furthermore, unlike the line-on-circle distortion effect (see Figure 11), but, again, like the triangle-to-square distortion effect (see Figure 21b), the magnitudes of the mouth-on-diamond distortion effects for the two spatial configurations did not differ significantly from each other, $F(1, 7) = 0.11, p < .8$.

As in the case of the triangle-on-square distortion effect, one might argue that for Configuration 1, the mouth pointing toward the diamond (the leftmost column in Figure 23) may be qualitatively distinct from the mouth pointing away from the diamond (the other left column in Figure 23). The strength of the distortion effect (in terms of the percentage of trials in which the observers saw the effect) in this case turned out to be marginally stronger for the priming mouth pointing away from the test diamond for both the flash trials and the motion trials. For the flash trials, the mean percentages of the shape-contrast responses were 74% ($SE = 9\%$) for the pointing-toward configuration and 93% ($SE = 2\%$) for the pointing-away configuration, the latter mean being almost significantly greater than the former, $F(1, 8) = 5.00$, $p < .06$. For the motion trials, the mean percentages were 79% ($SE = 7\%$) and 95% ($SE = 3\%$) for the two configurations, the latter mean being significantly greater than the former, $F(1, 8) = 5.97, p < .05$. Despite these differences, all four means were significantly above 50%, indicating that the shape-contrast effects were obtained for both subconfigurations for both the flash and the motion trials: $F(1, 8) = 7.61$, $p < .03$ for pointing toward in flash trials; $F(1, 8) = 374.49$, $p < .0001$ for pointing away in flash trials; $F(1, 8) = 16.31$, $p < .005$ for pointing toward in motion trials; and $F(1, 8) = 259.78, p < .0001$ for pointing away in motion trials.

Combined with the results obtained for the line-on-circle and triangle-on-square distortion effects, these results suggest that shape-contrast effects in general occur at the level of shape processing independently of spatial parameters. Particular spatial configurations of the interacting shapes, however, can modulate the magnitude of the distortion effects in some cases. Further research is needed to understand the configurational anisotropy found in this experiment and in Experiment 3 for the line-on-circle distortion effect.

General Discussion

We found reliable effects of shape contrast in the dimensions of aspect ratio (or elongation), taper, and curvature when a briefly flashed (and masked) stimulus was preceded by a prime of a shape differing in one of those dimensions

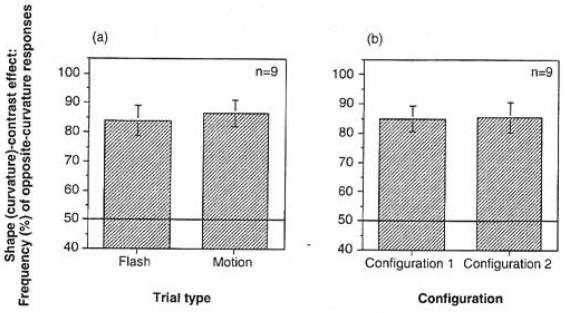

Figure 26. The curvature-contrast effect in Experiment 10. The y axis shows the proportion (%) of the responses consistent with the curvature-contrast effect (the test diamond appearing to be curved in the direction opposite to the curvature of the priming mouth). Thus, the values greater than 50% indicate a curvature-contrast effect, the values equal to 50% indicate no effect, and the values less than 50% indicate an unexpected "curvature-assimilation" effect. (a) Comparison between the flash trials and the motion trials. In the motion trials, the priming shape moved smoothly such that no apparent motion was seen from the priming shape to the test shape. The data are collapsed over the two configurations. (b) Comparison between Configurations 1 and 2 (refer to Figure 23). The data are collapsed over trial types (flash and motion). Error bars represent ± 1 SE for 9 observers.

and when the prime-to-test SOA was also brief (about 100–200 ms). An oriented line distorts a circle into an ellipse elongated along the orthogonal orientation. An isosceles triangle pointing to the right or left (see Figure 18) distorts the test square into a trapezoid tapered in the opposite direction. A mouthlike shape curving upward or downward (see Figure 22) makes the flattened test diamond appear curved in the opposite direction. The latter effects occurred despite the fact that the right- and left-pointing triangles were composed of an identical set of three line segments and the upward- and downward-curving mouths were composed of an identical set of four line segments. Thus, low-level contour interactions could not have produced those effects. The distortion effects occurred for large stimulus separations and for various stimulus configurations and were found independently of the perception of apparent motion from the priming stimulus to the test stimulus. On the basis of these findings, we think that we have demonstrated examples of pure shape-level (nonretinotopic) image interactions using briefly presented stimuli—the shape-contrast effect.

Note that the shape-contrast effect is orientation specific. The test circle always appears elongated perpendicular to the orientation of the priming line; thus, as the priming line is rotated by 90°, so is the axis of elongation of the test circle rotated by 90°. The test square always appears to be tapered in the direction opposite that in which the priming triangle is tapered; thus, as the priming triangle is rotated by 180° to point in the opposite direction, so is the direction of the distortion effect rotated by 180° such that the test square appears to be tapering off in the opposite direction.[16] The test diamond always appears curved in the direction opposite that in which the priming mouth is curved; thus, as the priming mouth is rotated by 180° to be curved in the opposite direction, so is the direction of the distortion effect rotated by 180° such that the test diamond appears curved in the opposite direction.

The presence of such shape-contrast effects implies the existence of a high-level image representation in which shapes are coded in figural dimensions in an orientation-specific manner, independently of retinotopic parameters such as spatial configuration, distance, and possibly scale.[17] We note that this description of a high-level shape representation closely resembles the response-tuning characteristics of the visual neurons found in the temporal lobe areas such as IT, where neurons show nonlocal but orientation-specific tunings for shapes (e.g., Tanaka, 1996; see our introduction). The possible link between the shape-contrast effects and the high-level visual processing in IT is further supported by a recent study by Rivest, Intriligator, Warner, and Suzuki (1997). They reported that line-on-circle[18] distortion effects occur with undiminished strength even if the priming line and the test circle are defined by two different surface attributes, one in equiluminant color and the other in luminance contrast. This finding is consistent with the fact that many IT cells respond to their preferred shapes defined by a range of color and luminance (Sato, Kawamura, & Iwai, 1980).

As discussed in our introduction, many IT and STS cells are known to have tunings for exemplars of a specific category of shapes (e.g., Perret et al., 1991—3-D views of faces; Hasselmo et al., 1989—facial expressions; Young & Yamane, 1992—face shapes; Fujita et al., 1992—various geometric shapes; Tanaka, 1996—various geometric shapes and 3-D views of faces). In particular, Fujita et al. (1992) and Tanaka (1996) found that some IT cells are organized into columns and that each column of cells exhibits response preferences for similar geometric shapes. Within a column, cells are tuned to different variations of the same preferred shape: slightly deformed, changed in orientation, reversed in contrast polarity, and so forth. We might speculate that the perception of tall and flattened ellipses, oppositely tapered trapezoids, and oppositely curved arcs might be mediated, respectively, by shape columns in which individual cells are tuned to ellipses of particular aspect ratios, trapezoids with particular directions and degrees of taper, and shapes with particular curvatures. The percept of a particular aspect ratio, taper, or overall curvature, then, could arise from the pattern of population activity of these aspect-ratio-tuned, taper-tuned, or curvature-tuned units in the respective shape space[19] such that the location of the centroid (or some other measure of the central tendency) of population activity determines the perceived shape.

In general, any attribute coded by a population-activity centroid, be it orientation, spatial frequency, position, direction of motion, or shape, is susceptible to a *repulsive* aftereffect in the corresponding coding dimension, given that active neurons are subjected to "fatigue" or a suppressive gain control (e.g., Sclar, Lennie, & DePriest, 1989; Wilson & Humanski, 1993) designed to calibrate the optimum range of neural responses to suit the given stimulus

[16] Although the distortion effects were tested only for the left-pointing and right-pointing triangles in Experiment 9, a pilot study showed that an upward/downward-pointing triangle also distorts the test square into a trapezoid tapering off in the opposite direction, that is, in the downward/upward-pointing direction.

[17] Rivest, Intriligator, Suzuki, and Warner (1998) recently reported that shape-contrast effects can occur across a large range of size differences between the priming and the test shapes. For example, using an ellipse (instead of a line) of a variable size as the priming stimulus, Rivest et al. obtained the aspect-ratio effect while the area ratio of the priming ellipse to the test circle (10.5 deg^2) was varied from about 1/10 to 3/1; the magnitude of the distortion effect showed broad tuning to size ratio. As for the neurons in IT, the degree of size tuning varies widely among the individual neurons (Tanaka, 1996), though so far no evidence has been found in IT of a systematic coding of size (like the columnar organization of size/spatial-frequency-tuned neurons in V1; e.g., Tootell et al., 1981, 1982).

[18] Elongated rectangles instead of lines were used as the priming stimuli.

[19] Shape space refers to a high-level image representation in which each location represents a particular shape. The metric of distance is the figural similarity; that is, shapes that are similar to one another are closer together and shapes that are dissimilar to one another are farther apart in shape space (e.g., Barlow, 1981). Retinal space, in contrast, refers to a low-level image representation in which each location represents a particular position on the retina. The distance in retinal space thus corresponds to the actual distance in the visual field in terms of visual angle.

environment. As discussed above, neurophysiological research suggests that in shape spaces, distances are measured in terms of figural similarity; for example, subjectively more similar shapes seem to be represented closer together, and more dissimilar shapes farther apart, in IT (e.g., Tanaka, 1996; Young & Yamane, 1992). Note that this is analogous to the way low-level features appear to be coded; similar orientations, spatial frequencies, and closer spatial locations are represented closer together in the primary visual cortex (e.g., Hubel & Weisel, 1968; Tootell, Silverman, & De Valois, 1981; Tootell, Silverman, Switkes, & De Valois, 1982), and similar directions of motion are represented closer together in MT (e.g., Albright et al., 1984). A shape-contrast effect can thus be considered as a repulsive aftereffect in a shape dimension, causing a test shape to appear "repelled away" from a priming shape in the direction of greater figural dissimilarity, just as tilt, size/spatial-frequency, figural, and motion aftereffects can be considered as repulsive aftereffects in the dimensions of orientation, spatial frequency, retinal location, and the direction of motion, respectively. In our examples, a priming line, a triangle, and a mouthlike shape with curvature "repel" geometrically symmetric test shapes further away from them in the respective figural dimensions, that is, in the direction of the opposite (or orthogonal) aspect ratio, the opposite taper, and the opposite curvature. In the following paragraphs we sketch a qualitative model of shape spaces (or shape columns, to use the analogy of the orientation columns in primary visual cortex, or V1) of aspect ratio, taper, and curvature to illustrate how response-based activity modulations of shape-tuned neurons can account for the shape-contrast effects we found.[20]

In Figure 27a, the seven humps in the lower graph represent the shape-tuning curves of seven hypothetical units in each of the three shape columns. In the aspect-ratio column, the units are tuned to a range of aspect ratios; in the taper column, the units are tuned to a range of directions and degrees of taper; in the curvature column, the units are tuned to a range of curvatures. These units might exist in IT or STS. In viewing Figure 27, it is interesting to note that tunings for aspect ratio, direction and degrees of taper, and curvature, may be interpreted, respectively, as tunings for different 3-D views (rotated in depth) of a flat disk, a rectangular plate, and a bent tube, which are analogous to the neural tunings for 3-D views of a head reported by Perret et al. (1991) and Tanaka (1996). Each unit responds most strongly when the stimulus falls on its peak sensitivity region, that is, when the stimulus shape coincides with the apex of its bell-shaped sensitivity curve. The response decreases as the stimulus shape deviates from the apex; no response occurs if the stimulus shape falls outside the area of the bell-shaped tuning curve. For example, the middle unit (Unit 4) is broadly tuned to "circle," "square," or "no curvature," and the leftmost unit (Unit 1) to "vertical line," "right-pointing triangle," or "upward curvature," in the respective three shape columns.

Suppose a circle, a square, or a flattened diamond with no net curvature is presented. The location of "circle," "square," or "no curvature" in the shape space of the corresponding shape column happens to be at the center of the receptive field of the middle unit (Unit 4). Unit 4 in each shape column would respond most strongly because its tuning curve intersects the stimulus at its peak; the strength of response is proportional to the height of the intersection. The tuning curves of the two adjacent units (Units 3 and 5) intersect the stimulus at slightly lower points, whereas the tuning curves of the next pair of adjacent units (Units 2 and 6) intersect the stimulus at much lower points. The tuning curves of the two most distant units (Units 1 and 7) never intersect the stimulus at all; thus, they would make no response. The pattern of population activity of the seven units thus obtained is shown by the gray curve. In this simple model, the location of the centroid (the vertical line that divides the population response curve into two equal areas) indicates the perceived shape of the stimulus. As is apparent from Figure 27a, the population response would be symmetric about the sensitivity peak of the middle unit (Unit 4), which corresponds to "circle," "square," or "no curvature" in the corresponding shape space (or column). Thus, the location of the centroid would also coincide with "circle," "square," or "no curvature," and therefore, the perceived shape of the stimulus would be veridical.

Now suppose a vertical priming line, a right-pointing priming triangle, or a mouthlike priming shape with net upward curvature was flashed prior to the corresponding test shape, a circle, a square, or a flattened diamond with no net curvature. The units on the left (Units 1 and 2) would respond particularly well to the priming shape. If this caused any suppressive effects on the subsequent responses of these units (be it fatigue or active gain control), as in the case of classic aftereffects, the pattern of population response to the test shape would skew toward the right. This would shift the population-activity centroid slightly to the right of the center to fall on "slightly horizontally elongated ellipse," "trapezoid slightly tapering off to the left," or "slight downward curvature" instead of falling on "circle," "square," or "no curvature" (see Figure 27b). Note that had the priming shape been a horizontal line, a left-pointing triangle, or a mouthlike shape with downward curvature, the centroid would then have shifted in the opposite direction (slightly to the left) to fall on "slightly vertically elongated ellipse," "trapezoid slightly tapering off to the right," or "slight upward curvature." These predictions are consistent with the shape-contrast effects obtained.

To summarize, our results provide strong evidence that a flashed priming shape distorts a subsequently flashed (and masked) test shape in a shape-contrasting way (in the direction of greater figural dissimilarity) over a wide range of spatial parameters given that the exposure duration of the test stimulus and the prime-to-test SOA are brief. The existence of such shape-contrast effects suggests that the coding of shapes at higher visual areas such as IT and STS may be analogous to the population coding of location, orientation, and spatial frequency in lower visual areas such as V1. However, the fact that the shape-contrast effects are

[20] Similar illustrations have been used by many to explain classic aftereffects (e.g., Braddick, Campbell, & Atkinson, 1978).

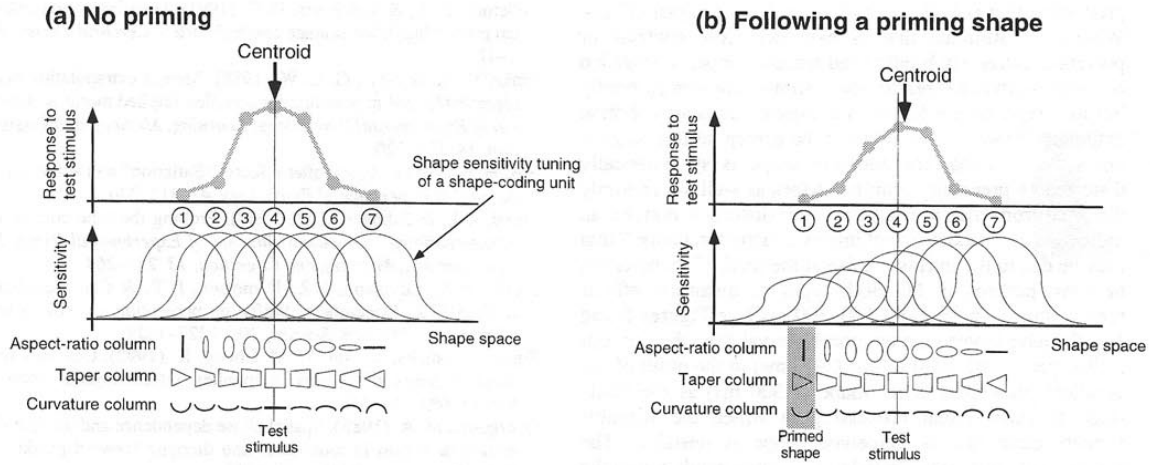

Figure 27. A possible explanation of the shape-contrast effect based on a graded response suppression of the shape-coding units that is in proportion to their responses to the priming stimulus. (a) In the lower graph, seven humps represent the shape tunings (receptive fields) of seven hypothetical units (Nos. 1–7) tuned to adjacent values of aspect ratio, taper, and curvature in the respective shape spaces (columns). The location of each numbered circle along the abscissa indicates the shape encoded by the corresponding unit. The gray points in the upper graph indicate the activity levels of these units in response to the test stimulus: circle, square, or elongated shape with no net curvature. The activity level of each unit is represented by the intersection of its tuning curve and the shape of the test stimulus (the middle vertical line). The location of the population-activity centroid (arrow) in the relevant shape space corresponds to the perceived shape. With no priming shape, the centroid coincides with the veridical shape of the test stimulus, namely, a circle, a square, or an elongated shape with no curvature, in this example. (b) Shorter humps around the primed shape (a vertical line, a right-pointing triangle, or an upward-curving mouth) represent the suppression of sensitivity induced by the priming shape in its vicinity. The centroid of the population response (arrow) is now shifted slightly to the right (away from the priming shape) so that the test circle is seen as a slightly horizontal ellipse, the test square as a trapezoid slightly tapered on the left, and the elongated test shape with no net curvature as being slightly downward curved—shape-contrast effects. Note that the population-activity centroid would be shifted to the left if the priming line was horizontal, the priming triangle was left pointing, or the priming mouth was downward curving.

only obvious at the labile stage of processing (the strong component of the effect rapidly diminishes during the first 150–300 ms of the test stimulus exposure) indicates that the effects of interactions between the shape-coding units are much less persistent than are those among low-level units responsible for classic aftereffects, which are observed under free viewing conditions.

On the basis of the shape-contrast effect, we found evidence that nonretinotopic representations of shape exist in at least three figural dimensions—aspect ratio, taper, and curvature. In our experiments, the specific stimulus shapes were chosen so that the distortion effects were most noticeable and most readily measurable. However, it is probably the case that the shape-contrast effects we found are fairly general and do not depend on the use of particular shapes as long as the priming and test stimuli are different along the dimensions of aspect ratio, taper, or curvature. For example, pilot results indicate that a square can be substituted for a circle as the test stimulus in the aspect-ratio (line-on-circle) contrast effect. We are currently examining the extent of this generality as well as looking for other figural dimensions, such as 3-D views of a face and facial expression, in which the shape-contrast effects may be found on the basis of the known shape tunings of the visual neurons in IT and STS.

In another direction of research, shape-contrast effects can be used to infer the tuning properties (width and symmetry of tuning; the tuning curves shown in Figure 27 are for a qualitative illustration only) of the "shape-tuned units" just as classic aftereffects have been used to infer the tuning characteristics of the retinotopic neural channels tuned to low-level image features (edge orientation, spatial frequency, and position; e.g., Blakemore & Campbell, 1969; Blakemore et al., 1970; Mitchell & Muir, 1976; O'Tool & Wenderoth, 1977; see Braddick et al., 1978, for a review). In a recent study, for example, Suzuki and Rivest (1998) used ellipses of a variety of aspect ratios as the priming and the test stimuli to determine the tuning properties of the aspect-ratio (line-on-circle) effect. Their finding suggests that the aspect-ratio-tuned units have broad and highly skewed tuning curves unlike the symmetric tuning curves shown in Figure 27.

In conclusion, we have identified a labile stage of visual

processing that is highly sensitive to shape-contrast effects. Whereas a stimulus that is extremely low contrast or presented extremely briefly (and masked) appears degraded or barely visible, a suprathreshold stimulus presented briefly but for longer than ~50 ms (and masked) appears coherent and clear. However, we find that the percept at this stage is not stable and that the apparent shape is systematically distorted by preceding priming shapes as well as randomly distorted from trial to trial; the latter distortion may be an indication of the existence of intrinsic "structural noise" that may be due to the intrinsic noise at the level of shape-tuned neurons, perhaps in IT. Both types of distortion effects remain strong up to about 150–300 ms (see Figures 6 and 14). We have labeled the temporal interval from the onset of a clear percept of the stimulus (~50 ms) to the onset of the veridical perception of its shape (~300 ms) as the labile stage of early visual processing in which the stimulus appears clear but its perceived shape is unstable. The perception at this stage provides a valuable window into the high-level neural interactions among shape-tuned units, which may reveal the underlying dimensions of shape coding.

References

Albright, T. D., Desimone, R., & Gross, C. G. (1984). Columnar organization of directionally selective cells in visual area MT of the macaque. *Journal of Neurophysiology, 51,* 16–31.

Anstis, S. M., & Moulden, B. P. (1970). After effect of seen movement: Evidence for peripheral and central components. *Quarterly Journal of Experimental Psychology, 22,* 222–229.

Barlow, H. B. (1981). Critical limiting factors in the design of the eye and visual cortex. *Proceedings of the Royal Society of London, Series B, 212,* 1–34.

Blakemore, C., & Campbell, F. W. (1969). On the existence of neurons in the human visual system selectively sensitive to the orientation and size of retinal images. *Journal of Physiology, 203,* 237–260.

Blakemore, C., Nachmias, J., & Sutton, P. (1970). The perceived spatial frequency shift: Evidence for frequency selective neurons in the human brain. *Journal of Physiology, 210,* 727–750.

Braddick, O., Campbell, F. W., & Atkinson, J. (1978). Channels in vision: Basic aspects. In R. Held, H. W. Leibowitz, & L.-H. Teuber (Eds.), *Handbook of sensory physiology: Vol. 8. Perception* (pp. 3–38). Berlin: Springer-Verlag.

Burt, P., & Sperling, G. (1981). Time, distance, and feature trade-offs in visual apparent motion. *Psychological Review, 88,* 171–195.

Cavanagh, P., & Mather, G. (1989). Motion: The long and short of it. *Spatial Vision, 4*(2/3), 103–129.

Culham, J. C., & Cavanagh, P. (1995). Motion aftereffects of attentive tracking are rotation-specific but independent of position. *Investigative Ophthalmology and Visual Science* (Suppl.), *36,* S857.

Desimone, R., & Gross, C. G. (1979). Visual areas in the temporal cortex of the macaque. *Brain Research, 178,* 363–380.

De Valois, R. L., Albrecht, D. G., & Thorell, L. G. (1982). Spatial frequency selectivity of cells in macaque visual cortex. *Vision Research, 22,* 545–559.

Eriksen, C. W., & Hoffman, M. (1963). Form recognition at brief duration as a function of adapting field and interval between stimulations. *Journal of Experimental Psychology, 65,* 485–499.

Felleman, D. J., & Van Essen, D. C. (1991). Distributed hierarchical processing in the primate cerebral cortex. *Cerebral Cortex, 1,* 1–47.

Finke, R. A., & Shyi, G. C.-W. (1988). Mental extrapolation and representational momentum for complex implied motions. *Journal of Experimental Psychology: Learning, Memory, and Cognition, 14,* 112–120.

Fox, H. B. (1951). Figural after-effects: "Satiation" and adaptation. *Journal of Experimental Psychology, 42,* 317–326.

Freyd, J. J., & Johnson, J. Q. (1987). Probing the time course of representational momentum. *Journal of Experimental Psychology: Learning, Memory, and Cognition, 13,* 259–268.

Frome, F. S., Levinson, J. Z., Danielson, J. T., & Clavadetscher, J. E. (1979, December). Shifts in perception of size after adaptation to gratings. *Science, 206,* 1327–1329.

Fujita, I., Tanaka, K., Ito, M., & Cheng, K. (1992). Columns for visual features of objects in monkey inferotemporal cortex. *Nature, 360,* 343–346.

Georgeson, M. A. (1988). Spatial phase dependence and the role of motion detection in monocular and dicoptic forward masking. *Vision Research, 28*(11), 1193–1205.

Georgeson, M. A., & Georgeson, J. M. (1987). Facilitation and masking of briefly presented gratings: Time course and contrast dependence. *Vision Research, 27,* 369–379.

Graziano, M. S., Andersen, R. A., & Snowden, R. J. (1994). Tuning of MST neurons to spiral motions. *Journal of Neuroscience, 14*(1), 54–67.

Gross, C. G., Rocha-Miranda, C. E., & Bender, D. B. (1972). Visual properties of neurons in inferotemporal cortex of the macaque. *Journal of Neurophysiology, 35,* 96–111.

Hammer, E. (1949). Temporal factors in figural after-effects. *American Journal of Psychology, 62,* 337–354.

Hartmann, L. (1955). Further studies of gamma movement. In W. D. Ellis (Ed.), *A source book of gestalt psychology.* New York: Humanities Press. (Original work published 1923)

Hasselmo, M. E., Rolls, E. T., & Baylis, G. C. (1989). The role of expression and identity in the face-selective responses of neurons in the temporal visual cortex of the monkey. *Experimental Brain Research, 32,* 203–218.

Helson, H. (1925). The psychology of gestalt. *American Journal of Psychology, 36,* 494–526.

Hubel, D. H., & Weisel, T. N. (1968). Receptive fields and functional architecture of monkey striate cortex. *Journal of Physiology, 195,* 215–243.

Ikeda, H., & Obatani, T. (1953). The quantitative analysis of figural after-effects: I. The process of growth and decay of figural after-effects. *Japanese Journal of Psychology, 23,* 246–260; *24,* 59–66.

Kelly, M. H., & Freyd, J. J. (1987). Explorations of representational momentum. *Cognitive Psychology, 19,* 369–401.

Kohler, W., & Wallach, H. (1944). Figural aftereffects: An investigation of visual processes. *Proceedings of the American Philosophical Society, 88,* 269–357.

Kolers, P. A. (1972). *International series in experimental psychology: Vol. 16. Aspects of motion perception.* Oxford, New York: Pergamon Press.

Korte, A. (1915). Kinematoskopische Untersuchungen. *Zeitschrift für Psycology, 72,* 193–296.

Lagae, L., Maes, H., Raiguel, S., & Xiao, D.-K. (1994). Responses of macaque STS neurons to optic flow components: A comparison of areas MT and MST. *Journal of Neurophysiology, 71*(5), 1597–1626.

Lindermann, E. (1955). Gamma movement. In W. D. Ellis (Ed.), *A source book of gestalt psychology.* New York: Humanities Press. (Original work published 1922)

Mitchell, D. E., & Muir, D. W. (1976). Does the tilt-aftereffect occur in the oblique meridian? *Vision Research, 16,* 609–613.

Movshon, J., Adelson, E., Gizzi, M., & Newsome, W. (1985). The analysis of moving visual patterns. In C. Chagas, R. Gattass, & C. Gross (Eds.), *Pattern recognition mechanisms* (pp. 117–151). New York: Springer-Verlag.

Newsome, W. T., Britten, K. H., & Movshon, J. A. (1989, September 7). Neuronal correlates of a perceptual decision. *Nature, 341,* 52–54.

Nijhawan, R. (1994, July 28th). Motion extrapolation in catching. *Nature, 370,* 256–257.

Ohyama, T. (1954). Experimental studies of figural aftereffects: II. Spatial factors. *Japanese Journal of Psychology, 25,* 195–206.

Ohyama, T. (1956). Experimental studies of figural aftereffects. III. Displacement effects. *Japanese Journal of Psychology, 26,* 365–375.

O'Tool, B., & Wenderoth, P. (1977). The tilt illusion: Repulsion and attraction effects in the oblique meridian. *Vision Research, 17,* 367–374.

Pelli, D. G. (1990). The quantum efficiency of human vision. In C. Blakemore (Ed.), *Vision: Coding and efficiency* (pp. 3–24). Cambridge, England: Cambridge University Press.

Perret, D. I., Oram, M. W., Harries, M. H., Bevan, R., Hietanen, J. K., Benson, P. J., & Thomas, S. (1991). Viewer-centered and object-centered coding of heads in the macaque temporal cortex. *Experimental Brain Research, 86,* 159–173.

Perret, D. I., Smith, P. A. J., Potter, D. D., Mistlin, A. J., Head, A. S., Milner, A. D., & Jeeves, M. A. (1984). Neurons responsive to faces in the temporal cortex: Studies of functional organizations, sensitivity to identity and relation to perception. *Human Neurobiology, 3,* 197–208.

Petersen, S. E., Baker, J. F., & Allman, J. M. (1985). Direction-specific adaptation in area MT of the owl monkey. *Brain Research, 346,* 146–150.

Regan, D., & Hamstra, S. J. (1992). Shape discrimination and the judgment of perfect symmetry: Dissociation of shape from size. *Vision Research, 32,* 1845–1864.

Rijsdijk, J., Kroon, J. N., & van der Wildt, G. J. (1980). Contrast sensitivity as a function of position on the retina. *Vision Research, 20,* 235–241.

Rivest, J., Intriligator, J., Suzuki, S., & Warner, J. (1998). A shape distortion effect that is size invariant. *Investigative Ophthalmology and Visual Science* (Suppl.), *39,* S853.

Rivest, J., Intriligator, J., Warner, J., & Suzuki, S. (1997). Color and luminance combine at a common neural site for shape distortions. *Investigative Ophthalmology & Visual Science* (Suppl.), *38,* S1000.

Rolls, E. T., Tovee, M. J., Purcell, D. G., Stewart, A. L., & Azzopardi, P. (1994). The responses of neurons in the temporal cortex of primates, and face identification and detection. *Experimental Brain Research, 101,* 473–484.

Sagara, M., & Ohyama, T. (1957). Experimental studies of figural aftereffects in Japan. *Psychological Bulletin, 54,* 327–338.

Sato, T., Kawamura, T., & Iwai, E. (1980). Responsiveness of inferotemporal single units to visual pattern stimuli in monkeys performing discrimination. *Experimental Brain Research, 38,* 313–319.

Saul, A. B., & Cynader, M. S. (1989a). Adaptation in single units in visual cortex: The tuning of aftereffects in the spatial domain. *Visual Neuroscience, 2,* 593–607.

Saul, A. B., & Cynader, M. S. (1989b). Adaptation in single units in visual cortex: The tuning of aftereffects in the temporal domain. *Visual Neuroscience, 2,* 609–620.

Sclar, G., Lennie, P., & DePriest, D. D. (1989). Contrast adaptation in striate cortex of macaque. *Vision Research, 29,* 747–755.

Sekuler, R., & Pantle, A. (1967). A model for after-effects of seen movement. *Vision Research, 7,* 427–439.

Spigel, I. M. (1962). Contour absence as a critical factor in the inhibition of the decay of a movement after-effect. *Journal of Psychology, 54,* 221–228.

Suzuki, S., & Cavanagh, P. (1997). Focused attention distorts visual space: An attentional repulsion effect. *Journal of Experimental Psychology: Human Perception and Performance, 23,* 443–463.

Suzuki, S., & Rivest, J. (1998). Interactions among "aspect-ratio channels." *Investigative Ophthalmology and Visual Science* (Suppl.), *39,* S855.

Tanaka, K. (1996). Inferotemporal cortex and object vision. *Annual Review of Neuroscience, 19,* 109–139.

Tanaka, K., & Saito, H. (1989). Analysis of motion of the visual field by direction, expansion/contraction, and rotation cells in the dorsal part of the medial superior temporal area of the macaque monkey. *Journal of Neurophysiology, 62,* 626–641.

Thompson, P. G., & Movshon, J. A. (1978). Storage of spatially specific threshold elevation. *Perception, 7,* 65–73.

Tootell, R. B. H., Reppas, J. B., Dale, A. M., & Look, R. B. (1995, May). Visual motion aftereffect in human cortical area MT revealed by functional magnetic resonance imaging. *Nature, 375* (6527), 139–141.

Tootell, R. B. H., Silverman, M. S., & De Valois, R. L. (1981). Spatial frequency columns in primary visual cortex. *Science, 214,* 813–815.

Tootell, R. B. H., Silverman, M. S., Switkes, E., & De Valois, R. L. (1982). The organization of cortical modules in primate striate cortex. *Society of Neuroscience Abstracts, 8,* 707.

Turvey, M. T. (1973). On peripheral and central processes in vision: Inferences from an information processing analysis of masking with patterned stimuli. *Psychological Review, 80,* 1–52.

von Grünau, M. W., & Dube, S. (1992). Comparing local and remote aftereffects. *Spatial Vision, 6,* 303–314.

Wassle, H., Grunert, U., Rohrenbeck, J., & Boycott, B. (1990). Retinal ganglion cell density and cortical magnification factor in the primate. *Vision Research, 30,* 1897–1911.

Wilson, H. R., & Humanski, R. (1993). Spatial frequency adaptation and contrast gain control. *Vision Research, 33,* 1133–1149.

Wohlgemuth, A. (1911). On the after-effect of seen movement. *British Journal of Psychology Monograph Supplement 1,* 1–117.

Wolfe, J. (1984). Short test flashes produce large tilt aftereffects. *Vision Research, 24,* 1959–1964.

Young, M. P., & Yamane, S. (1992). Sparse population coding of faces in the inferotemporal cortex. *Science, 256,* 1327–1331.

Received December 9, 1996
Revision received July 24, 1997
Accepted July 24, 1997 ■